Title: Age-related decline of synaptic plasticity is regulated by neuro-androgen and neuro-estrogen in normal aging of hippocampus

Suguru Kawato[1,2,3†], Yasushi Hojo[1,4], Mari Ogiue-Ikeda[1,2,3], Mika Soma[2,5], Minoru Saito[5], Jonghyuk Kim[1,2], Arisa Munetomo[1], Shimpei Higo[1], Hirotaka Ishii[1], Asami Kato[1], Hideo Mukai[1], Ayako Hiragushi[1], Takuji Shirasawa[6,7], Takahiko Shimizu[6,8] and Shigeo Horie[3]

[1]Department of Biophysics and Life Sciences, Graduate School of Arts and Sciences, The Univ. Tokyo, Tokyo, Japan.
[2]Department of Cognitive Neuroscience, Faculty of Pharma-Science, Teikyo Univ., Tokyo, Japan.
[3]Department of Urology, Graduate School of Medicine, Juntendo University, Tokyo, Japan.
[4]Department of Biochemistry, Saitama Medical University, Saitama, Japan.
[5]Department of Biosciences, College of Humanities and Sciences, Nihon University, Tokyo, Japan,
[6]Molecular Gerontology, Tokyo Metropolitan Institute of Gerontology, Tokyo, Japan.
[7]Department of Aging Control Medicine, Graduate School of Medicine, Juntendo University, Tokyo, Japan.
[8]Department of Mechanism of Aging, National Center for Geriatrics and Gerontology, Aichi, Japan.

[†]Correspondence: Suguru Kawato, e-mail : skkawato@gmail.com

Keywords aging, hippocampus, neuroandrogen, neuroestrogen, spine,

Abstract

We revealed a good relationship between age-dependent decrease in the hippocampal dendritic spine density and age-dependent decrease in hippocampal androgen and estrogen levels with normal aging of male rats.

Approximately 25% decrease in the spine density was observed in hippocampal CA1 region by going from 3 month-old (3m; young adult) to 24 month-old (24m; aged). We found a significant age-induced decrease in hippocampal neuro-androgen levels by going from 3m to 24 m using mass-spectrometric analysis. The hippocampal levels of testosterone (T) and dihydrotestosterone (DHT) dramatically decreased from 17 nM T and 7 nM DHT at 3 m to 17/100 nM T and 7/15 nM DHT at 24 m. On the other hand, hippocampal estradiol (E2) was moderately decreased with aging, from 8 nM at 3 m to

2 nM at 24m.

Comprehensive analysis of mRNAs of hippocampal steroidogenic enzymes and receptors showed an age-dependent decrease in their expression levels by approximately 50% (P450(17α)), 25% (17β-hydroxysteroid dehydrogenase) and 0% (5α-reductase and P450arom). Androgen receptor AR was moderately decreased but estrogen receptor ERα was not decreased with aging.

The 25% decrease in the spine density with aging may be due to a balance between considerably decreased T and DHT levels (spine decrease factor) and remained moderately high E2 level (spine increase factor) in the 24m hippocampus. Aged hippocampus still has moderate capacity of sex-steroid synthesis and their functions. Interestingly, DHT-supplementation and T-supplementation recovered the spine density at 24m.

1. Introduction

Our increasing life span is expected to decrease quality of life due to age-related declines in cognitive functions, due to not only pathological changes such as Alzheimer's disease (AD) but also normal aging.

In healthy humans, many literatures have described age-related perturbations in hippocampal activity coincident with deficits of learning and memory (Daselaar et al 2006) (Dennis et al 2008) (Beeri et al 2011).

Similarly, rodent models of normal aging demonstrate strong correlations between impaired performance of aged rats on behavioral tests of hippocampus-dependent learning and memory and decreased hippocampal neuron activity. The performance of spatial learning (dependent on CA1 region) and contextual fear learning (dependent on CA3 region) decline along with aging (Barnes 1987) (Burke & Barnes 2006) (Veng et al 2003). Age-dependent impairment of electrophysiological properties of hippocampal function is related to unstable encoding of spatial representations (Barnes et al 1997) (Kumar et al 2007) (Norris et al 1996) (Rosenzweig & Barnes 2003) (Wilson et al 2003) .

Aging-dependent pathological cognitive decline such as AD is a result of neuronal cell death or cell loss (Morrison & Hof 1997) (Morrison & Hof 2002) (West et al 1994). In case of normal aging, however, the number of neurons in the hippocampus and the cerebral cortex (CC) do not change along with aging (Burke & Barnes 2006) (Kelly et

al 2006) (Morrison & Hof 1997) (Morrison & Hof 2002) (Rapp & Gallagher 1996) (Rasmussen et al 1996) (West et al 2004).

These results suggest that the decline in the learning and memory with normal aging is likely to occur at a synaptic level, because of no neuron loss. Dendritic spines (post-synapses) in the hippocampus correlate with the performance of learning and memory. Increase in the density and the size of spines is associated with learning and memory tasks (Moser et al 1994, Moser et al 1997, O'Malley et al 2000). Structural synaptic plasticity is so important to study, because based on mounting evidence, it appears that growth of spines and formation of their synapses represent a morphological substrate for learning and memory (Kasai et al., 2003; Lang et al.,2004; Silva, 2003).

We focus on sex steroids as strong candidates for neurotrophic factors that correlate with aging effects on decline of the cognitive function in addition to reproductive system (Midzak et al 2009) (Chen et al 1994).

Decline in sex steroid, especially 17β-estradiol (E2), has been considered as an important factor which is involved in age-related female neural dysfunction, since E2 significantly decreases in plasma upon menopause that elicits cognitive decline and dysfunction of Hypothalamus-Pituitary-Gonadal axis (Kawakita et al 2021) (Kim et al 2017). The relationship between neural function and E2 has been extensively investigated in the male and female rodent hippocampus, including the modulatory effect of E2 on synaptic plasticity in CA1 region (Bi et al 2000) (Foy et al 1999) (Hasegawa et al 2015) (Mukai et al 2007) (Mukai et al 2010) (Ooishi et al 2012a) (Ooishi et al 2012b) (Vouimba et al 2000). The beneficial effects on dendritic spines by E2 replacement therapy have been investigated in aged female rodents and nonhuman primates (Hao et al 2007) (Hara et al 2015) (Morrison & Baxter 2012).

The mechanisms of androgen effects on synaptic plasticity have also attracted much attention. For example, perfusion of testosterone (T) and dihydrotestosterone (DHT) significantly increased dendritic spine density within 2 h in rat hippocampus slices (Hatanaka et al 2015). These rapid spine increases were driven by kinases via membrane synaptic AR receptor. T administration increases synaptic density in the dentate gyrus of aged mice (Fattoretti et al 2019). Castration of young male rats decreased serum T, and T replacement improved spatial memory (Wagner et al 2018). T replacement also improved spatial memory in aged male rats whose serum T level is low (Jaeger et al 2020). SAMP8 mouse is a senescence accelerated mouse which exhibits cognitive impairment and hypogonadism. Investigations of male SAMP8 mice showed the relationship between plasma T decline and age-related neural dysfunction

(Ota et al 2012). Interestingly, T and DHT replacement in male SAMP8 inhibited cognitive decline through an increase of sirtuin 1 protein (SIRT1) expression (Ota et al 2012). In relation to AD, apparent relationship between decrease in T level and progression of AD was observed in both human and rodents model of AD (Rosario et al 2004) (Rosario et al 2010).

Human data also indicate a significant decline in plasma T of men due to chronological aging (Harman et al 2001) (Morley et al 1997) (Travison et al 2007). Plasma T declines across the men's life span represents an issue of great concern for cognitive impairment. In many cases, the aging effects had been attributed to the decline in plasma T and E2, which are synthesized in testis and ovary (Janmaat et al 2011, Wu et al 2009). However, the hippocampus is able to locally synthesize sex steroids *de novo* in addition to the target of sex steroids (Fig. 1) (Hojo et al 2004) (Hojo et al 2008) (Kato et al 2013) (Kawato et al 2002) (Kimoto et al 2010).

Evidence of the role of hippocampus-s 2025ynthesized sex steroids in hippocampal function has been accumulated, including neurogenesis (Okamoto et al 2012), LTP (Di Mauro et al 2015, Di Mauro et al 2017, Grassi et al 2011) and memory consolidation (Tuscher et al 2016).

The purpose of the current study is, therefore, to demonstrate the relationship between age-related decrease in dendritic spines and aging-dependent decline in hippocampal sex steroidogenic systems. These investigations focus on hippocampal levels of androgen and estrogen as well as their receptors. We observed in the hippocampus, a good correlation between the aging-dependent decrease in the density of CA1 spines and the considerable decrease in androgen levels that reduced to ~1/100 fold by going from 3 month-old (3m, young adult) to 24 month-old (24m, old). The decrease was also observed in mRNA expression of androgen receptor (AR) and some androgen-synthesizing enzymes. The significant recovery of the spine density with androgen replacement at 24m hippocampus supports the capacity of hippocampal androgen that can prevent synaptic impairment with aging. Interestingly, the 24m hippocampal E2 level was only moderately decreased to 2 nM (1/4 fold of 3m hippocampus), and no decrease in P450arom (E2 synthase) and ERα expression was observed, suggesting that E2 can still support synaptic plasticity in the absence of androgen in aged hippocampus.

2. Results

2.1. Dendritic spines in CA1 pyramidal neurons

2.1.1. Age-induced decrease of spines

We investigated age-induced change in spine density and morphology of the hippocampal CA1 stratum radiatum, for 24m and 3m male rats (Fig. 2A). Spine analysis was performed for secondary branches of the apical dendrites located 100-200 μm away from the pyramidal cell body, in the middle of the stratum radiatum of CA1 region.

The total spine density showed age-induced decrease, from 2.29 spines/μm (3m) to 1.69 spines/μm (24m) which corresponds to approx. 26% decrease (Fig. 2B).

The morphological changes in spine head diameter were also assessed. Nearly 95 % of spines have clear heads and necks, and we classified the head diameter of spines into three categories: small-head spines (0.2–0.4 μm), middle-head spines (0.4–0.5 μm), and large-head spines (0.5-1.0 μm).

Along with aging, the density of all three types of spines was decreased. The density of large-head spines was decreased from 0.97 spines/μm (3m) to 0.68 spines/μm (24m) (Fig. 2C, 2D). The density of middle-head spines was decreased from 0.86 spines/μm (3m) to 0.73 spines/μm (24m). The density of small-head spines also decreased from 0.45 spines/μm (3m) to 0.28 spines/μm (24m).

2.1.2. Recovery of age-induced spine decrease by androgen administration

Upon single androgen administration for 24m rats, the spine density recovered after 17 h (Fig. 3A).

Total spine density analysis

DHT administration (1mg/kg) increased the total density of spines from 1.69 to 1.77 spines/μm ($F = 2.984$, $p = 0.009$, two-way ANOVA; $p = 0.0172$ for 24m vs 24m + DHT, Tukey-Kramer multiple comparison's test), which corresponds to approx. 5% increase. T administration (1mg/kg) increased the total spine density from 1.69 to 1.82 spines/μm ($F = 7.2224$, $p = 0.008$, two-way ANOVA; $p = 0.0392$ for 24m vs 24m + T, Tukey-Kramer multiple comparison's test), which corresponds to approx. 8% increase (Fig. 3B). Next, to clarify the involvement of androgen receptor (AR) in the recovery effect of androgen administration, we performed s.c. administration of flutamide (30 mg/kg), a specific antagonist against AR, 1 h before androgen administration. Co-administration of flutamide and DHT decreased the total spine density back to the control level (Fig. 3B). Co-administration of flutamide and T also decreased the total spine density back to the control level (Fig. 3B).

The additional effect of tamoxifen, an antagonist against estrogen receptor, to flutamide was investigated, because a part of T might be converted to estradiol. Simultaneous administration of tamoxifen (1 mg/kg) and flutamide (30 mg/kg) to T-injected group did not further decrease the total spine density of flutamide plus T injected group. As a control, no effect of flutamide alone (without androgen administration) was checked.

Spine head diameter analysis

The morphological changes in spine head diameter were also assessed. Upon DHT supplementation, small-head spines were significantly increased from 0.27 to 0.54 spines/μm ($p < 0.0001$ for small-head, Tukey-Kramer), while some decrease in large-head spines was observed (Figs. 3C1, 3D1). Upon T supplementation, small-head spines were mainly increased from 0.27 to 0.43 spines/μm ($p = 0.0468$ for small-head, Tukey-Kramer), without changes in middle-head and large-head spines (Figs. 3C2, 3D2). Co-administration of flutamide (Flu) and DHT blocked the DHT-induced increase of small-head spines and the DHT-induced decrease of large-head spines, without changing middle-head spines ($p < 0.0001$ for small-head, $p = 0.0002$ for large-head, Tukey-Kramer) (Figs. 3C1, 3D1). Co-administration of Flu and T blocked the T-induced increase of small-head spines ($p = 0.0273$ for small-head, Tukey-Kramer) (Figs. 3C2, 3D2).

2.2. Age-induced decrease in androgen and estrogen levels in the hippocampus from 3m to 12m and 24m

Mass-spectrometric analysis with LC-MS/MS was performed to accurately determine the change in levels of T, DHT and E2 with aging (Fig.4). The concentrations of T, DHT and E2 were determined by a chromatogram analysis of the fragmented ions of T-17-picolinoyl-ester, DHT-17-picolinoyl-ester and E2-3-pentafluorobenzyl (PFBz)-17-picolinoyl-ester, as shown in Supplementary figures (Fig. S1).

Importantly, if we use frozen hippocampal tissue, oxidation of 3-OH group of E2 by freeze-thaw processes-may cause artificial loss of E2 (Kawato et al 2025). We explain these problems in detail in Supplementary Methods. Therefore, we rapidly extract E2 from freshly separated hippocampal tissue by organic solvent. C18 column and HPLC are also useful for further purification of E2 from contaminating fats. High sensitivity detection was achieved by using picolinoyl derivatization (see Materials and Methods).

Data of steroid concentrations in 3m rats are taken from Hojo et al. (2009) (Hojo et al 2009).

In the hippocampus, the level of T monotonously decreased with age, from 17 ± 2.0 nM (3m) to 5.0 ± 0.9 nM (12m) and 0.2 ± 0.1 nM (24m) (Fig.4). The level of DHT also monotonously decreased with age, from 7.0 ± 2.0 nM (3m) and 2.0 ± 0.4 nM (12m) to 0.4 ± 0.07 nM (24m). The levels of T and DHT in 24m hippocampus extremely decreased to approximately 1% and 4% of those in 3m hippocampus.

The level of hippocampal E2 gradually decreased with age from 8.0± 1.0 (3m) to 8.0± 2.0 (12m) and 2.0 ± 0.5 nM (24m). The E2 level in 24m hippocampus was approx. 25% of that in 3m hippocampus.

Interestingly, the levels of T, DHT and E2 in 3m, 12m and 24 hippocampi were always higher than those in the plasma (Fig. 4). In the plasma, T level decreased from 11 ± 2.0 nM (3m) to 3.0 ± 0.7 nM (12m) and 0.3 ± 0.06 nM (24m). DHT level decreased with age, from 0.6 ± 0.09 nM (3m) to 0.1 ± 0.02 nM (12m) and 0.04 ± 0.004 nM (24m). The levels of T and DHT in 24m plasma were considerably low with approx. 3% and 7%, respectively, of those in 3m plasma. Male plasma E2 levels (0.01 nM at 3m, 0.02 nM at 12m and 0.03 nM at 24m) were always very low and did not show a significant change with aging.

2.3. Age-induced change in expression levels of mRNAs encoding sex-steroidogenic enzymes and sex steroid receptors

We performed the PCR analysis in the hippocampus (Hi) for male rats, which are aged 3 month (3m), 12 month (12m), and 24 month (24m). In the following the *italic* name (e.g., *Gapdh*) means the gene name of protein (e.g., GAPDH). The expression level of *Gapdh* mRNA did not show a significant age-related change over 3m, 12, and 24m (Fig. 5A). Therefore, in this section, all the expression levels of enzymes and receptors were normalized by the *Gapdh* level of 3m hippocampus, which was set to be 100%.

Furthermore, the levels of each enzyme and receptor were normalized by its enzyme and receptor levels in 3m hippocampus, which were set to be 100%, respectively.

2.3.1 Androgen synthesis enzymes and androgen receptor showed age-induced decrease (Figs. 5B-5F)

We investigated the expression levels of androgen synthesis enzymes, including DHEA synthase (P450(17α)), testosterone synthase [17β-hydroxysteroid dehydrogenase (17β-HSD) (1 and 3)], and DHT synthase (5α-reductase (1 and 2)). The level of *Cyp17a1* (mRNA of P450(17α)) decreased with age, from 100% (3m) to 62% (24m) (Fig. 5B). The level of *Hsd17b1* (mRNA of 17β-HSD1) decreased with age, from 100%

249 (3m) to 84% (24m) (Fig. 5C). The level of *Hsd17b3* decreased from 100% (3m) to 76%
250 (24m) (Fig. 4D). Although the *Srd5a1* level did not significantly change with age (Fig.
251 4E), the level of *Srd5a2* (mRNA of 5α-reductase 2) monotonously decreased from
252 100% (3m) to 85% (12%) to 75% (24m) (Fig. 5F).
253

254 **2.3.2. Estrogen synthesis enzyme did not change with age (Fig. 5G)**

255 The expression level of *Cyp19a1* (mRNA of P450arom) did not significantly show
256 age-related change (Fig. 4G), although the *Cyp19a1* level in 12m was a little bit higher
257 than those of 3m and 24m without statistical significance.

258 **2.3.3. Cholesterol transport, synthesis of pregnenolone (PREG) and progesterone**
259 **(PROG), in upstream of androgen and estrogen synthesis (Figs. 5H-5K)**

260 The level of *Star* (mRNA of steroidogenic acute regulatory protein (StAR))
261 decreased with age, from 100% (3m) to 75%, and 61% (24m) (Fig. 5H). Interestingly,
262 however, the level of *Tspo* (mRNA of translocator protein (TSPO)), monotonously
263 increased with age, from 100% (3m) to 111% (12m), and 127% (24m) (Fig. 5I).
264 Pregnenolone synthase *Cyp11a1* (mRNA of P450scc) and progesterone synthase *3β-*
265 *HSDI* (mRNA of 3β-HSD) were investigated. The expression levels of *Cyp11a1* and *3β-*
266 *HSDI* were much lower than levels of other sex steroid synthesis enzymes in
267 downstream. The *Cyp11a1* level decreased from 3m (100%) to 69% (24m) in average
268 (Fig. 5J). The age-dependent progressive decrease was observed for *3β-HSDI* level in
269 average (Fig. 5K). In individual experiments, mRNA was not observed (even with 42
270 PCR cycles) in 2 rats (12m) and 3 rats (24m), and observed in 2 rats (12m) and 1 rat
271 (24m) only, among 4 rats examined.
272

273 **2.3.4 Age dependence of androgen and estrogen receptors (Figs. 5L-5O)**

274 The expression level of androgen receptor, *Ar*, showed age-induced decrease from
275 100% (3m) to 85% (24m) (Fig. 5L). Although the level of *Esr1* (mRNA of ERα) did not
276 show age-induced change, the level of *Esr2* (mRNA of ERβ) monotonously decreased
277 from 100% (3m) to 87% (12m) to 62% (24m) (Figs. 5M, 5N). Interestingly, the *Pgr*
278 level (mRNA of progesterone receptor (PR)) did not change with age (Fig. 5O).
279

280 **2.3.5. Relative comparison of all the different enzymes and receptors at the same**
281 **age of hippocampus (Fig. 6)**

282 Fig. 6 shows comparison of relative expression levels of all the steroidogenic

enzymes and steroid receptors in the same age (24m, 12m and 3m), using equations explained in Methods section. We normalized by setting the level of *Cyp19a1* in 3m hippocampus to be 100%, because the expression level of *Cyp19a1* did not significantly change with age.

In order to have clear comparison of many enzymes and receptors whose expression levels are very different, 1/100 fold of *Srd5a1,* 1/50 fold of *Ar,* 1/10 fold of *Hsd17b1* are used for illustration in Fig. 6. Several interesting characteristics were observed at 24m. The expression level of *Srd5a1* was highest among all the enzymes examined. Second highest expression was the *Hsd17b3* level. The expression levels of *Ar* and *Esr1* were relatively high as compared with enzymes. The *Esr1* level was higher (by approxi.15 fold) than the *Esr2* level. The expression levels of *Cyp11a1* and *Hsd3b1* were extremely low among all the enzymes and receptors.

2.3.6. Neurotrophic factors *Bdnf* and senescence marker gene *Sirt1* and *Tp53* (Fig. S2)

Bdnf (mRNA of Brain-derived neurotrophic factor (BDNF) and *Brain Insulin-1* (mRNA of Brain Insulin-1) are typical neurotrophic factors in the hippocampus. The *Bdnf* expression level did not show age-related change. The *Brain Insulin-1* level increased with age, from 100% (3m) to 211% (24m). The expression level of *Brain Insulin-1* was much lower (approx. 1/8000) than that of *Bdnf* as judged from different amplification cycles (see Methods).

The *Sirt1* (mRNA of SIRT1, silent information regulator 1) and *Tp53* (mRNA of tumor protein 53) are senescence marker genes. The *Sirt1* level monotonously decreased from 100% (3m) to 80% (12m), and 61% (24m), however, the *Tp53* level did not show age-related change.

2.3.7. Immunostaining of hippocampal enzymes and receptors (Fig. S3)

The localization and expression levels of sex-steroidogenic enzymes and sex-steroid receptors in the hippocampus was investigated in 24m rats by using immunostaining with antibodies (Fig. S3). The characteristic image parameters were compared with those in 3m rats published in our earlier works (Kimoto et al 2001) (Kawato et al 2002) (Hojo et al 2004). Detailed explanation is described in **5.2 Supplementary Results** (Section: Immunostaining of hippocampal enzymes and receptors)**.**

3. Discussion

In the field of cognitive decline along with aging, a great volume of data have been accumulated, including aging-induced changes in neurons, synapses and neurotropic factors of the hippocampus and the prefrontal cortex in rodents and nonhuman primates (Buchman et al 2016) (Burke & Barnes 2006) (Hao et al 2007) (Hara et al 2015) (Morrison & Baxter 2012). Particularly, aging dependent dendritic spine loss in the hippocampal pyramidal neurons has been well examined (Dickstein et al 2013) (Hao et al 2006) (Morrison & Baxter 2012). However, neuronal alterations in relation to brain sex steroids not only with normal/healthy aging but also with pathological aging such as AD have not been sufficiently uncovered (Morrison & Baxter 2012) (Carroll et al 2010) (Rosario et al 2010). Therefore, the current observations give a significant contribution to understand what is going on along with healthy/normal aging of the hippocampus, through demonstration of the age-related correlations between the dendritic spine loss and sex-steroids properties (steroid levels, levels of mRNA and protein expression of sex steroidogenic enzymes/receptors). We particularly focused on local hippocampal sex steroids that are candidates for neuroprotective factors in aging and neurodegeneration, because changes in hippocampal sex steroid levels and their functions along with aging have not been extensively investigated.

3.1. Decrease in spine density and hippocampal sex steroids with normal aging

The current investigations have demonstrated that age-related degeneration in dendritic spines of male rat hippocampus have close relationships with the decline in androgen action and androgen levels. Along with aging from 3m to 24m, approx. 26% decrease in the total spine density was observed (Fig. 2). With aging, the density of all three types of spines was decreased, and the large-head spine population was most significantly decreased.

Androgen replacement was effective for recovery of the spine density. Sixteen hours after single DHT and T injection, individually, spine density was recovered by approx. 5~7 % via AR dependent mechanisms in 24m rat hippocampus (Fig. 3). These androgen replacements were significantly effective, because basal hippocampal levels of T and DHT was considerably decreased by going from 3m to 24m as observed by mass-spectroscopic analysis (Fig. 4). Surprisingly, the levels of DHT and T in 24m hippocampus was only approx. 4% and 1%, respectively, of those in 3m hippocampus. These low androgen cases could be assigned to a kind of “andropose state”. This andropose-like state may appear due to not only considerable decrease of testis-derived

354 androgen but also particularly low DHEA production in rat adrenal cortex (containing
355 very low level of cytochrome P450(17α)) which is entirely different from human
356 adrenal cortex that could produce significant level of DHEA even at aged state.
357 Why the total spine density in 24m hippocampus was maintained at the moderately
358 high density (approx.74% of that of 3m), even with no androgen ? One reason may be
359 that the E2 level in 24m hippocampus was still moderately high, approxi.1/4 level of
360 that in 3m, which is effective to keep the moderately high spine density (Hasegawa et al
361 2015) (Mukai et al 2010). Another reason could be that neurotrophic factors,
362 including brain-derived neurotrophic factor (BDNF), nerve growth factor (NGF)
363 (Perovic et al 2013) and Brain-insulin, were not at all decreased with aging in the
364 hippocampus. These neurotrophic factors are important candidates which could increase
365 spines (Pozzo-Miller et al 1999) and elevate LTP (Kramar et al 2004), but no age-
366 induced decrease in their levels imply no contribution to the observed spine density
367 decline.
368 It is well known that in AD model mice such as 3xTg-AD and Tg2576 mice, the
369 spine density decreased considerably with aging. These spine degenerations are
370 explained through the effects of Aβ oligomers and Aβ plaque (Bittner et al 2010)
371 (Jacobsen et al 2006), therefore. the cause of spine decrease is very different from
372 healthy aging.
373
374 **3.2. Hippocampal synthesis capacity of androgen and estrogen in aged rats**
375
376 Until the current investigations, aging-dependence of local androgen and estrogen
377 synthesis systems after adult stages were poorly understood in not only the
378 hippocampus but also other brain regions. Our earlier study (Munetomo et al 2015)
379 described aging dependence of mRNAs of representative steroidogenic P450s and
380 hydroxysteroid-dehydrogenase (HSD) in the hypothalamus (Hy), the Cerebral Cortex
381 (CC) and the Cerebellum (CL). StAR immunostaining had been exceptionally shown in
382 aged rat hippocampal neurons at 24m (Sierra et al 2003).
383 Local androgen synthesis capacity from PROG to T and DHT depending on
384 P450(17α) and 17β-HSD (1,3) was significantly decreased with aging (Figs. 4, 5),
385 however their mRNA expression levels of *Cyp17a1* and *Hsd17b1,3* in 24m
386 hippocampus still keep approx. 50% − 75% of those in 3m hippocampus. Therefore,
387 local androgen synthesis activity from PROG to T through androstenedione in 24m
388 hippocampus might not be lower than 50% of that in 3m hippocampus (see synthesis
389 pathway in Fig. 1).

390 However, only a very low level of T (0.2 nM) was observed in 24 hippocampus.
391 Under the assumption that local T synthesis capacity from PROG (see Fig. 1) may be
392 maintained at around 50% as deduced from mRNA levels, why hippocampal T level
393 was extremely low in 24m ? One reason of age-dependent considerable decrease in
394 hippocampal T and DHT levels (Fig. 4) is probably a considerable decrease in
395 penetration of circulating T to the hippocampus (down to approx. 3%, by going from
396 3m to 24m), because circulating T penetrates/permeates into the hippocampus and
397 circulating T accounts for approx. 70 - 80% of hippocampal T, as observed in Fig. 3A
398 and our earlier studies (Hojo et al 2009). It should be noted that circulating DHT level is
399 much lower than hippocampal DHT level (less than 10% of hippocampal DHT level)
400 (Fig. 4), and therefore circulating DHT cannot contribute to maintain hippocampal DHT
401 level. The hippocampal DHT level was maintained by local conversion from
402 hippocampal T (Hojo et al 2009). Another reason of low hippocampal T could be
403 explained as a very efficient local conversion of T to DHT (by 5α-reductase) and T to
404 E2 (by P450arom). T to DHT conversion may be very efficient, because the expression
405 level of 5α-reductase in the hippocampus was the highest among all steroidogenic
406 enzymes (Figs. 4 and 5) and no age dependent decrease was observed for 5α-reductase.
407 Indeed, these efficient rapid conversion from T to DHT and 3a-androstanediol were
408 observed at 3m hippocampus (Hojo et al 2009) (Hojo et al 2011).
409 T to E2 conversion may also be efficient, because the mRNA level of P450arom did
410 not decrease with aging. Note that no ^{3}H-E2 degradation was observed within the
411 hippocampal slices, implying that E2 is very stably present once synthesized (Hojo et al
412 2004).
413 Interestingly, E2 synthesis capacity was only moderately decreased even at 24m.
414 *Cyp19* and P450arom immunostaining did not decrease, and therefore the E2 level in
415 24m hippocampus was still kept ~1/4 of that in 3m. Penetration of circulating E2 to the
416 hippocampus cannot contribute, because plasma E2 level is always lower than
417 hippocampus E2 level.
418 The above considerations are based on the sufficient PROG supply to the
419 hippocampus via blood PROG circulation at 24m (Valle et al 2008), and this is
420 supported by the results that plasma PROG level was increase from 6m to 24m in male
421 rats (Valle et al 2008). This is an important point, because local PROG synthesis
422 capacity from cholesterol may be very poor in 24m hippocampus, because expression
423 levels of P450scc and 3β-HSD1 were very low as judged from mRNAs and
424 immunostaining (Fig. 5 and Supplementary Fig. S3).
425 P450scc mRNA expression level was much lower than mRNAs of other androgen

and estrogen synthases. P450scc protein staining was considerably decreased at 24m. 3β-HSD1 mRNA was nearly negligible at 24m. In 3m hippocampus, mRNA expression of 3β-HSD1 was observed for all the 10 rats examined. However, in 24m rats 3β-HSD1 mRNA was not observed in 3 rats (24m), among 4 rats examined. Note that only averaged data are shown in Fig. 4 for 24m. These results imply the almost negligible conversion from PREG to PROG (and from DHEA to T) via 3β-HSD1. From these considerations, aged rat hippocampus needs circulating PROG as an initial precursor steroid for T synthesis, and this is supported by the sufficient level of circulating PROG at 24m (Valle et al 2008).

3.3. Comparison between androgen and estrogen receptors with healthy aging of hippocampus

AR expression level was decreased with aging, however the mRNA expression level in 24m hippocampus still keep approx. 85% of that in 3m hippocampus (Fig. 5). On the other hand, T and DHT levels were extremely low in the 24m hippocampus. Therefore, T and DHT supplementation could significantly recover the spine density via AR (Fig. 2). No significant decline was observed in the levels of estrogen receptor ERα with aging (Fig. 5), in contrast to the decrease of AR. Although ERβ mRNA decreased with aging (Fig. 5) (Yamaguchi & Yuri 2012), this ERβ decrease might not significantly alter the synaptic plasticity of the hippocampus. One reason is that the ERβ expression level is only around 10% of ERα expression level (Fig. 5). Another reason is that much smaller contributions of ERβ than those of ERα to spinogenesis and LTP were observed in earlier studies (Hasegawa et al 2015) (Phan et al 2011) (Phan et al 2015). ERα agonist PPT upregulated spinogenesis and LTP-induction upon weak theta-burst stimulation but ERβ agonist DPN did not show any effects.

Together with no decrease in estrogen synthesis enzyme P450arom, these results suggest that estrogen signaling could still well regulate synaptic plasticity even in aged 24m hippocampus.

3.4. No neuron loss but synaptic protein decrease in normal aging

The number of neurons in the hippocampus does not change in healthy aging of rodents, even for rats with impairment of special learning (Rapp & Gallagher 1996) (West et al 1994, West et al 2004). Also no neuron loss occurred in CC via healthy aging (Burke & Barnes 2006) (Kelly et al 2006) (Morrison & Hof 1997) (Morrison & Hof 2002). The number of neurons did not significantly decrease in prefrontal cortex (Peters et al 1994, Smith et al 2004) (Peters et al 1998), visual cortex (Kim et al 1997, Vincent

et al 1989), and entorhinal cortex (Gazzaley et al 1997, Merrill et al 2001) of rodents and primates. Therefore, the cognitive deficits, which occurred in healthy aged animals, might be due to decrease in synapses, but not loss of number of neurons. No change in the number of neurons also occurs in Hy during normal aging (Roberts et al 2012). On the other hand, the number of Purkinje cells in CL decreases due to aging (Janmaat et al 2011, Woodruff-Pak et al 2010).

Examination of possible age-induced decrease in hippocampal synaptic proteins is essential for understanding of impairment of cognition. NMDA glutamate receptors (Avila et al 2017, Magnusson et al 2010) and postsynaptic density protein 95 (PSD-95) (Fig. S3) (VanGuilder et al 2011) showed considerable decrease with age, which is a strong evidence for the decline in synaptic plasticity such as LTP with aging.

3.5. No reduction in typical endogenous neurotrophic factors

Neurotrophic factors play important roles in synaptic plasticity, maintenance of neural activity and neuroprotection. Importantly in the hippocampus, no age dependent changes in representative neurotrophic factors such as BDNF and NGF have been indicated (Fig. S2) (Croll et al 1998) (Perovic et al 2013).

In Hy and CL, BDNF protein and mRNA level also did not significantly change with age (Munetomo et al 2015) (Ewa et al 2012, Katoh-Semba et al 1998, Perovic et al 2013, Silhol et al 2005).

Brain-Insulin is an another neurotrophic factor (Gerozissis 2003) (de la Monte & Wands 2005). Brain-Insulin increased by going from 3m to 24m in the hippocampus (Fig. S2). Brain-Insulin showed the similar age-dependent increase also in other brain regions including CC, Hy and CL.

These results imply that the currently observed age-dependent spine decrease in the hippocampus cannot be caused by these typical neurotrophic factors, including BDNF and NGF. In AD, although BDNF decreased (Buchman et al 2016), NGF increased (Scott et al 1995). Therefore, age dependent changes in brain neurotrophic factors should be carefully considered.

3.6. Age-dependent changes of AR, ER and steroidogenic enzymes in non-hippocampal brain regions

Age-dependent changes of steroid receptors and steroidogenic enzymes showed very different tendency in different brain regions, including the hippocampus, Hy, CC and CL in rats. We discuss typical differences between hippocampus and other regions (Hy, CC, CL) in details in **5.3 Supplementary Discussion**.

498

499 **3.7. Characteristics of hippocampal synaptic degeneration in AD model animals,**
500 **different from normal aging**

501 Changes in synaptic plasticity and alterations of hippocampal neurons have been
502 extensively investigated in AD model mice as a typical model of pathological aging.
503 Very different from healthy aging, amyloid β (Aβ) plaques and
504 hyperphosphorylated tau are main factors that affect synapses in AD model mice
505 including triple transgenic AD mice (3xTg-AD) which progressively develop both Aβ
506 and tau pathology in the hippocampus (Bittner et al 2010). In the hippocampus of 3xTg-
507 AD male mice, dendritic spine density declines at 15 months (15m) at which Aβ
508 plaques are abundant (Bittner et al 2010).
509 Sex-steroids may play a role in neuroprotection in 3xTg-AD mice (Carroll et al 2010)
510 (Rosario et al 2010). In 3xTg-AD male mice, a significant increase in Aβ accumulation
511 in hippocampus was observed in gonadectomized (GDX) mice. Treatment of GDX
512 mice with T or DHT (for 4 m, from 3 m of age until 7 months of age) prevented the
513 increased Aβ accumulation in the hippocampus. E2 also prevented Aβ accumulation in
514 the hippocampus. Levels of tau hyperphosphorylation slightly increased by GDX.
515 Treatment of GDX mice with T and E2 but not DHT reduced tau hyperphosphorylation.
516 These data suggest that T can suppress Aβ pathology through androgen and estrogen
517 pathways and can reduce tau pathology largely through estrogen pathways.
518 Another type of AD model mice is Tg2576 mice which are human amyloid
519 precursor protein (APP) transgenic mice lines. In our preliminary investigations, a
520 significant spine loss of the total spine density was observed in CA1 region of the
521 hippocampus of 12m Tg2576 female mice, using the 3-dimentional confocal imaging of
522 Lucifer yellow injected hippocampal neurons. From morphology analysis, large-head
523 spines were particularly decreased without significant loss of middle- and small-head
524 spines. The loss of the total spine density in Tg2576 female mice was also observed at
525 6m and 12m using Golgi stained 2-dimentional analysis (Ricobaraza et al 2012). In
526 Tg2576 male mice, spine loss in dentate gyrus (DG) region was observed at 4m and 12
527 m using Golgi stained 2-dimentional analysis, however a significant Aβ increase was
528 observed from 18 m (Jacobsen et al 2006). In Tg2576 male, both long-term potentiation
529 (LTP) deficits in hippocampal CA1 and DG and spatial memory deficits in a modified
530 water maze were observed at 6 m. Although Aβ plaques did not develop until 18 m
531 (Hsiao et al 1996), both LTP deficits in hippocampal CA1 and DG and spatial memory
532 deficits in a modified water maze were detected at 6 m. Taken together, these results
533 imply that impaired synaptic plasticity appears before Aβ plaque formation (Chapman

et al 1999), therefore normally aged states of 24m hippocampus with spine loss might be similar to pre- Aβ plaque states of AD model animals.

3.8. Comparison between semi-quantitative PCR and real-time PCR

We can obtain essentially the same information from the current semi-quantitative PCR method (Hojo et al 2004) (Kimoto et al 2010) and real-time PCR (Munetsuna et al 2009). In order to perform normalization, both methods need to choose a good standard house-keeping gene, which must not change with age in addition to region-independent expression. The real-time PCR also cannot avoid these processes. We observed that *Gapdh* satisfied these criteria. Since the expression levels of mRNAs for steroidogenic enzymes are extremely low in the adult brain (Hojo et al 2004) (Kimoto et al 2010) , the primer design is most important. Concerning primer design of steroidogenic enzymes and receptors (with specificity and selectivity), dependent on free energy calculation, our semi-quantitative PCR methods are much more optimized (from many experiences) than real-time PCR (with fewer experiences) (Munetsuna et al 2009). Taken together, as far as we choose the PCR cycle number within the exponential amplification phase, we can achieve essentially the same results between semi-quantitative PCR method and real-time PCR method.

4. Materials and Methods

4.1. Animals

Male Wistar rats of 3, 12, 24-month-old were used in the current study. Animals were housed in the animal facility of Tokyo Metropolitan Institute of Gerontology, under a 12 h-light / dark cycle and were allowed *ad libitum* access to food and water. All experiments were performed with the approval of the Committee for Animal Research of the University of Tokyo.

4.2. Chemicals

DHT and T and Lucifer Yellow were purchased from Sigma-Aldrich (USA). E2, Flutamide and Tamoxifen were from Fujifilm-Wako Chemical (Japan).

Picolinic acid was from Tokyo Chemical Industry (Japan) and [1,2,3,4-$^{13}C_4$]E_2 was from Hayashi Pure Chemical (Japan). T-d_3 and DHT-d_3 were from CDN Isotope Inc. (Canada). [3H] labeled steroids ([2,4,6,7-^{3}H]-E2, [1,2,6,7-^{3}H]-T, and [1,2,6,7-^{3}H]-DHT)

were purchased from Perkin Elmer (USA).

4.3. Hippocampal spine analysis

Subcutaneous drug administration of animals

DHT (1 mg/kg body weight), T (1 mg/kg body weight), E2 (40 μg/kg body weight), Flu (mg/kg body weight) and Tamoxifen (mg/kg body weight) was dissolved in sesame oil to reach its appropriate concentration. The final volume was adjusted to 400 μl. Subcutaneous administration was performed at 5 pm which was 17 h before the decapitation. During the administration, the rats were gently handled by the experimenter.

Slice preparation (from in vivo fixed hippocampus)

Hippocampal slices were prepared from a 12-week-old male rat that was deeply anesthetized and perfused transcardially with PBS (0.1 M phosphate buffer and 0.14 M NaCl, pH 7.3), followed by a fixative solution of 3.5% paraformaldehyde. Immediately after decapitation, the brain was removed from the skull and post-fixed with the fixative solution. The dorsal hippocampus was then dissected and 400 μm thick transverse slices to the long axis, from the middle third of the hippocampus, were prepared with a vibratome (Dosaka, Japan).

Imaging and analysis of dendritic spine density and morphology

Current injection of Lucifer Yellow

Neurons within slices were visualized by an injection of Lucifer Yellow under a Nikon E600FN microscope (Japan) equipped with a C2400-79H infrared camera (Hamamatsu Photonics, Japan) and 40× water immersion lens (Nikon). A glass electrode was filled with 4% Lucifer Yellow, which was then injected for 5 min using Axopatch 200B (Axon Instruments, USA). With this process, approx. five neurons within a 10–20 μm depth from the surface of a slice were injected.

Confocal laser microscopic imaging and analysis

The imaging was performed from sequential z-series scans with LSM5 PASCAL confocal microscope (Zeiss, Germany) at high zoom (3.0) with a 63× water immersion lens, NA 1.2 (Zeiss). For Lucifer Yellow, the excitation and emission wave lengths were 488 nm and 530 nm, respectively. For analysis of spines, three-dimensional image was reconstructed from approximately 30 sequential z-series sections for every 0.45 μm. The

applied zoom factor (3.0) yielded 23 pixels per 1 μm. The confocal lateral resolution was approximately 0.16 μm. The z-axis resolution was approximately 0.47 μm. The confocal lateral resolution was approximately 0.16 μm. The z-axis resolution was approximately 0.47 μm. Our resolution limits were regarded to be sufficient to allow the determination of the head diameter of spines in addition to the density of spines. Confocal images were then deconvoluted using AutoDeblur software (AutoQuant, USA).

The density of spines as well as the head diameter were analyzed with Spiso-3D (automated software calculating mathematically geometrical parameters of spines) developed by Bioinformatics Project of Kawato's group (Mukai et al 2011). Spiso-3D has an equivalent capacity with Neurolucida (MicroBrightField, USA), furthermore, Spiso-3D considerably reduces human errors and experimenter labor. The single apical dendrite was analyzed separately. The spine density was calculated from the number of spines along secondary dendrites having a total length of 40-60 μm. These dendrites were present within the stratum radiatum, between 100-200 μm from the soma.

Spine shapes were classified into three categories as follows: (1) small-head spines, with a head diameter between 0.2-0.4 μm; (2) middle-head spines, which have 0.4-0.5 μm spine heads; and (3) large-head spines, with a head diameter between 0.5 and 1.2 μm. The reason of this classification depends on the consideration that these three types of spines may have different efficiency in signal transduction. Small-, middle-, and large-head spines probably have different number of α-amino-3-hydroxy-5-methyl-4-isoxazolepropionic acid (AMPA) receptors, and therefore these three types of spines might have different efficiency in memory storage. The number of AMPA receptors (including GluR1 subunits) in the spine increases as the size of postsynapse increases, whereas the number of N-methyl-D-aspartate (NMDA) receptors (including NR2B subunits) might be relatively constant (Shinohara et al 2008). Because the majority of spines (> 93 %) had a distinct head, and stubby spines and filopodia did not contribute much to overall spine distribution, we analyzed spines having a distinct head.

4.4. Mass-spectrometric assay of steroids

Detailed procedures are described in our earlier publications (Hojo et al 2009) and **5.1 Supplementary methods**. Briefly, the analysis consists of three steps described in the following:

First Step: Purification of steroids from hippocampi with normal phase HPLC

We performed sequential preparations, including homogenization of freshly isolated hippocampal tissues (not frozen-thawed tissues), organic solvent extraction of steroids, removal of fats with C18 column, and purification of T, DHT, E2 with normal phase HPLC (Hojo et al 2009). Importantly in frozen-thawed tissues, oxidation of 3-OH group of E2 may cause artificial modification of E2, because attack by reactive oxygens species (produced from mitochondria) may occur in freezing and thawing processes because of leaking and losing of antioxidants (such as glutathione and vitamin C) and antioxidant enzymes (such as superoxide dismutase and glutathione peroxidase) due to braking of cell membranes by crystallization of intracellular water and melting of intracellular ice. Therefore, we rapidly extract E2 from freshly separated hippocampal tissue by organic solvent (ethyl acetate/hexane).

Second Step: Derivatization of HPLC-purified steroids before application to LC (reverse-phase)-MS/MS

We prepared T-17-picolinoyl-ester, DHT-17-picolinoyl-ester and E2-pentafluorobenzyl (PFBz)-17-picolinoyl-ester by derivatization of T and DHT and E2 (Hojo et al 2009) (Hojo et al 2011). Derivatized T, DHT and E2 with picolinoyl is useful for induced-ionization by electron spray of MS/MS. Derivatization of E2 with pentafluorobenzyl is useful for improving evaporation efficiency by electron spray.

Third Step: Determination of the concentration for T, DHT and E2 using LC-MS/MS

For determination of the concentration of T, DHT and E2, the liquid chromatography-tandem mass spectrometry (LC-MS/MS) system, which consists of a Shimadzu LC system and POI-5000 triple stage quadrupole mass spectrometer (Applied Biosystems, USA) were employed. In the multiple reaction monitoring mode, the instrument monitored the m/z transition, from 394 to 253 for T-picolinoyl, from 396 to 203 for DHT-picolinoyl and from 558 to 339 for E2-PFBz-picolinoyl, respectively (see Fig. S1). Isotope-labeled steroid derivatives were used for internal standards in order to calibrate the retention time as well as measure recovery of steroids.

The limits of quantification for steroids were measured with blank samples, prepared alongside hippocampal samples through the whole extraction, fractionation and purification procedures. The limits of quantification for T, DHT, E2 were 1 pg, 1 pg, 0.3 pg per 0.1g of hippocampal tissue or 1 mL of plasma, respectively (Table S1). From the calibration curve using standard steroids dissolved in blank samples, the good linearity was observed.

675 **4.5. Molecular biological analysis of steroidogenic enzymes and steroid receptors**

676 **Total RNA isolation**

677 Rats were deeply anesthetized and were decapitated. The hippocampi were quickly
678 removed and immersed in ice-cold artificial cerebrospinal fluid (pH 7.4, 290 mOsm),
679 and stored in liquid nitrogen until use. Total RNA was extracted using SV Total
680 Isolation System (Promega, USA) according to the manufacturer's instructions. Total
681 RNA was then treated with Recombinant DNase I (RNase-free DNase I; Takara, Japan),
682 and then purified. The concentration was quantified by absorption at 260 and 280 nm.

683 **Primer design (Table S2AB)**

684 Since the expression of steroidogenic enzymes and steroid receptors is extremely
685 low in the brain, PCR primers with high sensitivity and specificity were carefully
686 designed for precise analysis (Kimoto et al 2010). We designed the primers considering
687 Gibbs energy (ΔG) as follows:
688 (1) ΔG of the whole primer ($\Delta G_{(whole)}$) was calculated with a nearest-neighbor model,
689 and set to be below the mean value for all of the primer candidates (ΔG_{av}) to obtain
690 good stability in primer-target interaction. (2) ΔG of the five 3'-terminal bases of the
691 primer ($\Delta G_{(5base)}$) was set to be higher than ΔG_{av} for improved specificity.
692 Consequently, ΔG of 5'-terminal bases was set to be less than the ΔG_{av}, resulting not
693 only in the improved stability in 5'-terminal interaction but also in the improved DNA
694 polymerase recognition. Two (forward and reverse) primers were designed on separate
695 exons and primers were designed to avoid 'PCR debris' including primer dimers.

696 **RT-PCR**

697 Semi-quantitative PCR was performed essentially as described in our earlier study
698 (Hojo et al 2004) (Kimoto et al 2010). As we explain in Discussion 4.9., we can obtain
699 essentially the same information from the current semi-quantitative PCR method and
700 real-time PCR (Munetsuna et al 2009).
701 The amount of cDNA, the number of PCR cycles, and the sequences of
702 oligonucleotide primers used in RT-PCR are shown in Supplementary Table S2A, S2B.
703 For RT, total RNA was reverse-transcribed into first-strand cDNA using an
704 oligo(dT) primer. Reaction solution (25 μL) contained 10 μg of total RNA, 1x RT
705 buffer, 1 mM dNTP mixture, 2 μg oligo$(dT)_{15}$ (Promega, USA), 40 U RNasin *Plus*
706 (Promega), and 200 U RTase (Toyobo, Japan). The reaction was carried out at 42°C for
707 60 min, and stopped by heating 75°C for 15 min. cDNA was treated with 4 U RNase H

708 (Takara bio, Japan) at 37°C for 30 min, and stored at -20°C until use.
709 PCR was performed in 25 μL of PCR mixture comprising cDNA corresponding to
710 100 ng of total RNA, 1 x PCR buffer, 0.2 M dNTP mixture, 0.2 μM forward and reverse
711 primers, and 0.63 U Blend Taq polymerase (Toyobo, Japan). PCR was performed with
712 cycle reactions at 95°C for 30 sec, 56-68°C for 20 sec, and 72°C for 30 sec, with an
713 initial denaturing at 95°C for 2 min and a final elongation at 72°C for 5 min. The PCR
714 products were applied to 2% agarose gels. Gels were stained with ethidium bromide
715 (EtBr) and visualized under UV light. Fluorescence images were recorded with
716 Printgraph (ATTO, Japan). For quantitative estimation, images of the bands were
717 analyzed using the Image J software (National Institutes of Health, Bethesda, MD). In
718 all the cases, we first plotted amplification curves in order to obtain the exponential
719 amplification phase of PCR plot.

720 **DNA sequencing**

721 PCR products were extracted from agarose gels using a Wizard SV Gel and PCR
722 Clean-up System (Promega) and cloned into pGEM-T-Easy vectors (Promega, USA).
723 Sequencing reactions were performed using a BigDye Terminator v3.1 Cycle
724 Sequencing Kit (Applied Biosystems, Foster City, CA, USA). Signals were detected
725 using an ABI PRISM 3130 Genetic Analyzer (Applied Biosystems, USA). In all the
726 expression analyses, the sequence identity between PCR products and target sequences
727 was confirmed with DNA sequencing.

728 **Comparison of the mRNA levels for different enzymes and receptors**

729 We used the comparison method for mRNA levels of different enzymes/receptors
730 obtained by using different primers (Kimoto et al 2010). Relative abundance of different
731 genes was estimated by adopting the expression level of glyceralaldehyde-3-phosphate
732 dehydrogenase mRNA (*Gapdh*) as an internal standard. Optical density value in each
733 band was divided by the number of $(1+e)^c$, where c is a PCR cycle number and e is an
734 amplification efficacy obtained from the PCR amplification curves in the exponential
735 amplification phase. More theoretical details were described in (Kimoto et al 2010).
736

737 **4.6. Immunohistochemistory**

738 Immunohistochemical staining was performed essentially as described in our
739 earlier studies (Kimoto et al 2001) (Hojo et al 2004). The hippocampi were frozen-
740 sliced with a cryostat. After application of primary antibody, the slices were incubated
741 for 16-48 h. Primary antibodies used are rabbit anti-P450scc IgG (aa421-

441,Chemicon) (1:200), rabbit anti-StAR IgG (PA1-560), Affinity BioReagents) (1:500), rabbit anti-AR IgG (PG-21, Millipore) (1:5000), rabbit anti-ERα IgG (1:1000), rabbit anti-guinea pig P450(17α) IgG (Shinzawa et al 1988) (1:1000), rabbit anti-human P450arom IgG (Jakab et al 1993) (1:1000), and mouse monoclonal anti-PSD95 IgG (ab2723, abcam) (1:1000). For secondary antibody, biotinylated goat anti-rabbit IgG and streptavidin-horseradish peroxidase complex (Vector Lab.) were applied. For mouse monoclonal antibody, biotinylated anti-mouse IgG was used as secondary antibody. Immunoreactive cells were detected with diaminobenzidine-nickel staining.

4.7. Statistical analysis of hippocampal dendritic spines and mRNA expression

For dendritic spine analysis, drug-treated dendrite images were used for spine analysis, and typical images were shown in Figs 2 and 3. Each dendrite has approx. 50 μm in length including approx. 75-120 spines. In Figs 2 and 3, for each steroid and inhibitor administration analysis of 24m rat dendritic spines, we used 3 rats, 12 slices, 24 neurons, 48 dendrites, and approx. 4100 spines. For statistical analysis of spines in Fig.2, we employed two-way ANOVA, followed by Tukey-Kramer multiple comparison's test.

For statistical analysis of age dependent changes of steroid levels in Fig.4 and mRNA expressions in Figs.5 and S2, we employ one-way ANOVA, followed by Tukey-Kramer multiple comparison's test.

764 References

765

766 Avila J, Llorens-Martín M, Pallas-Bazarra N, Bolós M, Perea JR, et al. 2017. Cognitive
767 Decline in Neuronal Aging and Alzheimer's Disease: Role of NMDA Receptors and
768 Associated Proteins. *Frontiers in Neuroscience* 11
769 Barnes CA. 1987. Neurological and behavioral investigations of memory failure in aging
770 animals. *Int J Neurol* 21-22: 130-6
771 Barnes CA, Rao G, Shen J. 1997. Age-related decrease in the N-methyl-D-aspartateR-
772 mediated excitatory postsynaptic potential in hippocampal region CA1. *Neurobiology*
773 *of aging* 18: 445-52
774 Beeri MS, Lee H, Cheng H, Wollman D, Silverman JM, Prohovnik I. 2011. Memory activation
775 in healthy nonagenarians. *Neurobiology of aging* 32: 515-23
776 Bi R, Broutman G, Foy MR, Thompson RF, Baudry M. 2000. The tyrosine kinase and mitogen-
777 activated protein kinase pathways mediate multiple effects of estrogen in
778 hippocampus. *Proc Natl Acad Sci U S A* 97: 3602-7
779 Bittner T, Fuhrmann M, Burgold S, Ochs SM, Hoffmann N, et al. 2010. Multiple events lead
780 to dendritic spine loss in triple transgenic Alzheimer's disease mice. *PLoS One* 5:
781 e15477
782 Buchman AS, Yu L, Boyle PA, Schneider JA, De Jager PL, Bennett DA. 2016. Higher brain
783 BDNF gene expression is associated with slower cognitive decline in older adults.
784 *Neurology* 86: 735-41
785 Burke SN, Barnes CA. 2006. Neural plasticity in the ageing brain. *Nature reviews.*
786 *Neuroscience* 7: 30-40
787 Carroll JC, Rosario ER, Kreimer S, Villamagna A, Gentzschein E, et al. 2010. Sex differences
788 in b-amyloid accumulation in 3xTg-AD mice: role of neonatal sex steroid hormone
789 exposure. *Brain Res* 1366: 233-45
790 Chapman PF, White GL, Jones MW, Cooper-Blacketer D, Marshall VJ, et al. 1999. Impaired
791 synaptic plasticity and learning in aged amyloid precursor protein transgenic mice.
792 *Nat Neurosci* 2: 271-6
793 Chen H, Hardy MP, Huhtaniemi I, Zirkin BR. 1994. Age-related decreased Leydig cell
794 testosterone production in the brown Norway rat. *J Androl* 15: 551-7
795 Croll SD, Ip NY, Lindsay RM, Wiegand SJ. 1998. Expression of BDNF and trkB as a function
796 of age and cognitive performance. *Brain Res* 812: 200-8
797 Daselaar SM, Fleck MS, Dobbins IG, Madden DJ, Cabeza R. 2006. Effects of healthy aging
798 on hippocampal and rhinal memory functions: an event-related fMRI study. *Cereb*
799 *Cortex* 16: 1771-82

800 de la Monte SM, Wands JR. 2005. Review of insulin and insulin-like growth factor expression,
801 signaling, and malfunction in the central nervous system: relevance to Alzheimer's
802 disease. *J Alzheimers Dis* 7: 45-61
803 Dennis NA, Hayes SM, Prince SE, Madden DJ, Huettel SA, Cabeza R. 2008. Effects of aging
804 on the neural correlates of successful item and source memory encoding. *J Exp*
805 *Psychol Learn Mem Cogn* 34: 791-808
806 Di Mauro M, Tozzi A, Calabresi P, Pettorossi VE, Grassi S. 2015. Neo-synthesis of estrogenic
807 or androgenic neurosteroids determine whether long-term potentiation or depression
808 is induced in hippocampus of male rat. *Front Cell Neurosci* 9: 376
809 Di Mauro M, Tozzi A, Calabresi P, Pettorossi VE, Grassi S. 2017. Different synaptic
810 stimulation patterns influence the local androgenic and estrogenic neurosteroid
811 availability triggering hippocampal synaptic plasticity in the male rat. *Eur J*
812 *Neurosci* 45: 499-509
813 Dickstein DL, Weaver CM, Luebke JI, Hof PR. 2013. Dendritic spine changes associated with
814 normal aging. *Neuroscience* 251: 21-32
815 Ewa BS, Beata L, Ilona K, Dariusz S, Janusz M. 2012. Brain derived neurotrophic factor
816 (BDNF) containing neurons in the hypothalamic paraventricular and supraoptic
817 nuclei of juvenile and middle-aged rats after chronic stress. *International journal of*
818 *developmental neuroscience : the official journal of the International Society for*
819 *Developmental Neuroscience* 30: 139-46
820 Fattoretti P, Malatesta M, Mariotti R, Zancanaro C. 2019. Testosterone administration
821 increases synaptic density in the gyrus dentatus of old mice independently of physical
822 exercise. *Exp Gerontol* 125: 110664
823 Foy MR, Xu J, Xie X, Brinton RD, Thompson RF, Berger TW. 1999. 17beta-estradiol enhances
824 NMDA receptor-mediated EPSPs and long-term potentiation. *J Neurophysiol* 81:
825 925-9
826 Gazzaley AH, Thakker MM, Hof PR, Morrison JH. 1997. Preserved number of entorhinal
827 cortex layer II neurons in aged macaque monkeys. *Neurobiology of aging* 18: 549-53
828 Gerozissis K. 2003. Brain insulin: regulation, mechanisms of action and functions. *Cell Mol*
829 *Neurobiol* 23: 1-25
830 Grassi S, Tozzi A, Costa C, Tantucci M, Colcelli E, et al. 2011. Neural 17beta-estradiol
831 facilitates long-term potentiation in the hippocampal CA1 region. *Neuroscience* 192:
832 67-73
833 Hao J, Rapp PR, Janssen WG, Lou W, Lasley BL, et al. 2007. Interactive effects of age and
834 estrogen on cognition and pyramidal neurons in monkey prefrontal cortex. *Proc Natl*
835 *Acad Sci U S A* 104: 11465-70

836 Hao J, Rapp PR, Leffler AE, Leffler SR, Janssen WG, et al. 2006. Estrogen alters spine
837 number and morphology in prefrontal cortex of aged female rhesus monkeys. *J*
838 *Neurosci* 26: 2571-8
839 Hara Y, Waters EM, McEwen BS, Morrison JH. 2015. Estrogen Effects on Cognitive and
840 Synaptic Health Over the Lifecourse. *Physiol Rev* 95: 785-807
841 Harman SM, Metter EJ, Tobin JD, Pearson J, Blackman MR. 2001. Longitudinal effects of
842 aging on serum total and free testosterone levels in healthy men. Baltimore
843 Longitudinal Study of Aging. *J Clin Endocrinol Metab* 86: 724-31
844 Hasegawa Y, Hojo Y, Kojima H, Ikeda M, Hotta K, et al. 2015. Estradiol rapidly modulates
845 synaptic plasticity of hippocampal neurons: Involvement of kinase networks. *Brain*
846 *Res*
847 Hatanaka Y, Hojo Y, Mukai H, Murakami G, Komatsuzaki Y, et al. 2015. Rapid increase of
848 spines by dihydrotestosterone and testosterone in hippocampal neurons: Dependence
849 on synaptic androgen receptor and kinase networks. *Brain Res* 1621: 121-32
850 Hojo Y, Hattori TA, Enami T, Furukawa A, Suzuki K, et al. 2004. Adult male rat hippocampus
851 synthesizes estradiol from pregnenolone by cytochromes P45017alpha and P450
852 aromatase localized in neurons. *Proc Natl Acad Sci U S A* 101: 865-70
853 Hojo Y, Higo S, Ishii H, Ooishi Y, Mukai H, et al. 2009. Comparison between hippocampus-
854 synthesized and circulation-derived sex steroids in the hippocampus. *Endocrinology*
855 150: 5106-12
856 Hojo Y, Higo S, Kawato S, Hatanaka Y, Ooishi Y, et al. 2011. Hippocampal synthesis of sex
857 steroids and corticosteroids: essential for modulation of synaptic plasticity. *Front*
858 *Endocrinol (Lausanne)* 2: 43
859 Hojo Y, Murakami G, Mukai H, Higo S, Hatanaka Y, et al. 2008. Estrogen synthesis in the
860 brain--role in synaptic plasticity and memory. *Mol Cell Endocrinol* 290: 31-43
861 Hsiao K, Chapman P, Nilsen S, Eckman C, Harigaya Y, et al. 1996. Correlative memory
862 deficits, Abeta elevation, and amyloid plaques in transgenic mice. *Science* 274: 99-
863 102
864 Jacobsen JS, Wu CC, Redwine JM, Comery TA, Arias R, et al. 2006. Early-onset behavioral
865 and synaptic deficits in a mouse model of Alzheimer's disease. *Proc Natl Acad Sci U*
866 *S A* 103: 5161-6
867 Jaeger ECB, Miller LE, Goins EC, Super CE, Chyr CU, et al. 2020. Testosterone replacement
868 causes dose-dependent improvements in spatial memory among aged male rats.
869 *Psychoneuroendocrinology* 113: 104550
870 Jakab RL, Horvath TL, Leranth C, Harada N, Naftolin F. 1993. Aromatase immunoreactivity
871 in the rat brain: gonadectomy-sensitive hypothalamic neurons and an unresponsive

872 "limbic ring" of the lateral septum-bed nucleus-amygdala complex. *J Steroid Biochem*
873 *Mol Biol* 44: 481-98
874 Janmaat S, Akwa Y, Doulazmi M, Bakouche J, Gautheron V, et al. 2011. Age-related Purkinje
875 cell death is steroid dependent: RORalpha haplo-insufficiency impairs plasma and
876 cerebellar steroids and Purkinje cell survival. *Age (Dordr)* 33: 565-78
877 Kato A, Hojo Y, Higo S, Komatsuzaki Y, Murakami G, et al. 2013. Female hippocampal
878 estrogens have a significant correlation with cyclic fluctuation of hippocampal spines.
879 *Front Neural Circuits* 7: 149
880 Katoh-Semba R, Semba R, Takeuchi IK, Kato K. 1998. Age-related changes in levels of brain-
881 derived neurotrophic factor in selected brain regions of rats, normal mice and
882 senescence-accelerated mice: a comparison to those of nerve growth factor and
883 neurotrophin-3. *Neurosci Res* 31: 227-34
884 Kawakita T, Yasui T, Yoshida K, Matsui S, Iwasa T. 2021. Correlations of androstenediol with
885 reproductive hormones and cortisol according to stages during the menopausal
886 transition in Japanese women. *J Steroid Biochem Mol Biol* 214: 106009
887 Kawato S, Hojo Y, Kimoto T. 2002. Histological and metabolism analysis of P450 expression
888 in the brain. *Methods Enzymol* 357: 241-9
889 Kawato S, Ogiue-Ikeda M, Soma M, Horie S, Saito M, Minato K. 2025. Rethinking synthesis
890 and function of neuro-estrogen and neuro-androgen in the hippocampus: some
891 methodological problems and possible solutions. *bioRxiv*
892 Kelly KM, Nadon NL, Morrison JH, Thibault O, Barnes CA, Blalock EM. 2006. The
893 neurobiology of aging. *Epilepsy Res* 68 Suppl 1: S5-20
894 Kim C, Harlow SD, Zheng H, McConnell DS, Randolph JF, Jr. 2017. Changes in
895 androstenedione, dehydroepiandrosterone, testosterone, estradiol, and estrone over
896 the menopausal transition. *Womens Midlife Health* 3
897 Kim CB, Pier LP, Spear PD. 1997. Effects of aging on numbers and sizes of neurons in
898 histochemically defined subregions of monkey striate cortex. *The Anatomical record*
899 247: 119-28
900 Kimoto T, Ishii H, Higo S, Hojo Y, Kawato S. 2010. Semicomprehensive analysis of the
901 postnatal age-related changes in the mRNA expression of sex steroidogenic enzymes
902 and sex steroid receptors in the male rat hippocampus. *Endocrinology* 151: 5795-806
903 Kimoto T, Tsurugizawa T, Ohta Y, Makino J, Tamura H, et al. 2001. Neurosteroid synthesis
904 by cytochrome p450-containing systems localized in the rat brain hippocampal
905 neurons: N-methyl-D-aspartate and calcium-dependent synthesis. *Endocrinology*
906 142: 3578-89
907 Kramar EA, Lin B, Lin CY, Arai AC, Gall CM, Lynch G. 2004. A novel mechanism for the

908 facilitation of theta-induced long-term potentiation by brain-derived neurotrophic
909 factor. *J Neurosci* 24: 5151-61
910 Kumar A, Thinschmidt JS, Foster TC, King MA. 2007. Aging effects on the limits and
911 stability of long-term synaptic potentiation and depression in rat hippocampal area
912 CA1. *J Neurophysiol* 98: 594-601
913 Magnusson KR, Brim BL, Das SR. 2010. Selective Vulnerabilities of N-methyl-D-aspartate
914 (NMDA) Receptors During Brain Aging. *Frontiers in aging neuroscience* 2: 11
915 Merrill DA, Chiba AA, Tuszynski MH. 2001. Conservation of neuronal number and size in
916 the entorhinal cortex of behaviorally characterized aged rats. *The Journal of*
917 *comparative neurology* 438: 445-56
918 Midzak AS, Chen H, Papadopoulos V, Zirkin BR. 2009. Leydig cell aging and the mechanisms
919 of reduced testosterone synthesis. *Mol Cell Endocrinol* 299: 23-31
920 Morley JE, Kaiser FE, Perry HM, 3rd, Patrick P, Morley PM, et al. 1997. Longitudinal
921 changes in testosterone, luteinizing hormone, and follicle-stimulating hormone in
922 healthy older men. *Metabolism* 46: 410-3
923 Morrison JH, Baxter MG. 2012. The ageing cortical synapse: hallmarks and implications for
924 cognitive decline. *Nature reviews. Neuroscience* 13: 240-50
925 Morrison JH, Hof PR. 1997. Life and death of neurons in the aging brain. *Science* 278: 412-9
926 Morrison JH, Hof PR. 2002. Selective vulnerability of corticocortical and hippocampal circuits
927 in aging and Alzheimer's disease. *Progress in brain research* 136: 467-86
928 Moser MB, Trommald M, Andersen P. 1994. An increase in dendritic spine density on
929 hippocampal CA1 pyramidal cells following spatial learning in adult rats suggests
930 the formation of new synapses. *Proc Natl Acad Sci U S A* 91: 12673-5
931 Moser MB, Trommald M, Egeland T, Andersen P. 1997. Spatial training in a complex
932 environment and isolation alter the spine distribution differently in rat CA1
933 pyramidal cells. *The Journal of comparative neurology* 380: 373-81
934 Mukai H, Hatanaka Y, Mitsuhashi K, Hojo Y, Komatsuzaki Y, et al. 2011. Automated Analysis
935 of Spines from Confocal Laser Microscopy Images: Application to the Discrimination
936 of Androgen and Estrogen Effects on Spinogenesis. *Cereb Cortex*
937 Mukai H, Kimoto T, Hojo Y, Kawato S, Murakami G, et al. 2010. Modulation of synaptic
938 plasticity by brain estrogen in the hippocampus. *Biochim Biophys Acta* 1800: 1030-
939 44
940 Mukai H, Tsurugizawa T, Murakami G, Kominami S, Ishii H, et al. 2007. Rapid modulation
941 of long-term depression and spinogenesis via synaptic estrogen receptors in
942 hippocampal principal neurons. *J Neurochem* 100: 950-67
943 Munetomo A, Hojo Y, Higo S, Kato A, Yoshida K, et al. 2015. Aging-induced changes in sex-

944 steroidogenic enzymes and sex-steroid receptors in the cortex, hypothalamus and
945 cerebellum. *The journal of physiological sciences : JPS* 65: 253-63
946 Munetsuna E, Hojo Y, Hattori M, Ishii H, Kawato S, et al. 2009. Retinoic Acid Stimulates 17
947 beta-Estradiol and Testosterone Synthesis in Rat Hippocampal Slice Cultures.
948 *Endocrinology* 150: 4260-69
949 Norris PJ, Faull RL, Emson PC. 1996. Neuronal nitric oxide synthase (nNOS) mRNA
950 expression and NADPH-diaphorase staining in the frontal cortex, visual cortex and
951 hippocampus of control and Alzheimer's disease brains. *Brain Res Mol Brain Res* 41:
952 36-49
953 O'Malley A, O'Connell C, Murphy KJ, Regan CM. 2000. Transient spine density increases in
954 the mid-molecular layer of hippocampal dentate gyrus accompany consolidation of a
955 spatial learning task in the rodent. *Neuroscience* 99: 229-32
956 Okamoto M, Hojo Y, Inoue K, Matsui T, Kawato S, et al. 2012. Mild exercise increases
957 dihydrotestosterone in hippocampus providing evidence for androgenic mediation of
958 neurogenesis. *Proc Natl Acad Sci U S A* 109: 13100-5
959 Ooishi Y, Kawato S, Hojo Y, Hatanaka Y, Higo S, et al. 2012a. Modulation of synaptic
960 plasticity in the hippocampus by hippocampus-derived estrogen and androgen. *J*
961 *Steroid Biochem Mol Biol* 131: 37-51
962 Ooishi Y, Mukai H, Hojo Y, Murakami G, Hasegawa Y, et al. 2012b. Estradiol rapidly rescues
963 synaptic transmission from corticosterone-induced suppression via
964 synaptic/extranuclear steroid receptors in the hippocampus. *Cereb Cortex* 22: 926-36
965 Ota H, Akishita M, Akiyoshi T, Kahyo T, Setou M, et al. 2012. Testosterone deficiency
966 accelerates neuronal and vascular aging of SAMP8 mice: protective role of eNOS and
967 SIRT1. *PLoS One* 7: e29598
968 Perovic M, Tesic V, Mladenovic Djordjevic A, Smiljanic K, Loncarevic-Vasiljkovic N, et al.
969 2013. BDNF transcripts, proBDNF and proNGF, in the cortex and hippocampus
970 throughout the life span of the rat. *Age (Dordr)* 35: 2057-70
971 Peters A, Leahu D, Moss MB, McNally KJ. 1994. The effects of aging on area 46 of the frontal
972 cortex of the rhesus monkey. *Cereb Cortex* 4: 621-35
973 Peters A, Sethares C, Moss MB. 1998. The effects of aging on layer 1 in area 46 of prefrontal
974 cortex in the rhesus monkey. *Cereb Cortex* 8: 671-84
975 Phan A, Lancaster KE, Armstrong JN, MacLusky NJ, Choleris E. 2011. Rapid effects of
976 estrogen receptor alpha and beta selective agonists on learning and dendritic spines
977 in female mice. *Endocrinology* 152: 1492-502
978 Phan A, Suschkov S, Molinaro L, Reynolds K, Lymer JM, et al. 2015. Rapid increases in
979 immature synapses parallel estrogen-induced hippocampal learning enhancements.

Proc Natl Acad Sci U S A 112: 16018-23

Pozzo-Miller LD, Inoue T, Murphy DD. 1999. Estradiol increases spine density and NMDA-dependent Ca2+ transients in spines of CA1 pyramidal neurons from hippocampal slices. *J Neurophysiol* 81: 1404-11

Rapp PR, Gallagher M. 1996. Preserved neuron number in the hippocampus of aged rats with spatial learning deficits. *Proc Natl Acad Sci U S A*

Rasmussen T, Schliemann T, Sorensen JC, Zimmer J, West MJ. 1996. Memory impaired aged rats: no loss of principal hippocampal and subicular neurons. *Neurobiology of aging* 17: 143-7

Ricobaraza A, Cuadrado-Tejedor M, Marco S, Perez-Otano I, Garcia-Osta A. 2012. Phenylbutyrate rescues dendritic spine loss associated with memory deficits in a mouse model of Alzheimer disease. *Hippocampus* 22: 1040-50

Roberts DE, Killiany RJ, Rosene DL. 2012. Neuron numbers in the hypothalamus of the normal aging rhesus monkey: stability across the adult lifespan and between the sexes. *The Journal of comparative neurology* 520: 1181-97

Rosario ER, Carroll J, Pike CJ. 2010. Testosterone regulation of Alzheimer-like neuropathology in male 3xTg-AD mice involves both estrogen and androgen pathways. *Brain Res* 1359: 281-90

Rosario ER, Chang L, Stanczyk FZ, Pike CJ. 2004. Age-related testosterone depletion and the development of Alzheimer disease. *Jama* 292: 1431-2

Rosenzweig ES, Barnes CA. 2003. Impact of aging on hippocampal function: plasticity, network dynamics, and cognition. *Prog Neurobiol* 69: 143-79

Scott SA, Mufson EJ, Weingartner JA, Skau KA, Crutcher KA. 1995. Nerve growth factor in Alzheimer's disease: increased levels throughout the brain coupled with declines in nucleus basalis. *J Neurosci* 15: 6213-21

Shinohara Y, Hirase H, Watanabe M, Itakura M, Takahashi M, Shigemoto R. 2008. Left-right asymmetry of the hippocampal synapses with differential subunit allocation of glutamate receptors. *Proc Natl Acad Sci U S A* 105: 19498-503

Shinzawa K, Ishibashi S, Murakoshi M, Watanabe K, Kominami S, et al. 1988. Relationship between zonal distribution of microsomal cytochrome P-450s (P-450(17)alpha,lyase and P-450C21) and steroidogenic activities in guinea-pig adrenal cortex. *J Endocrinol* 119: 191-200

Sierra A, Lavaque E, Perez-Martin M, Azcoitia I, Hales DB, Garcia-Segura LM. 2003. Steroidogenic acute regulatory protein in the rat brain: cellular distribution, developmental regulation and overexpression after injury. *Eur J Neurosci* 18: 1458-67

1016 Silhol M, Bonnichon V, Rage F, Tapia-Arancibia L. 2005. Age-related changes in brain-
1017 derived neurotrophic factor and tyrosine kinase receptor isoforms in the hippocampus
1018 and hypothalamus in male rats. *Neuroscience* 132: 613-24
1019 Smith DE, Rapp PR, McKay HM, Roberts JA, Tuszynski MH. 2004. Memory impairment in
1020 aged primates is associated with focal death of cortical neurons and atrophy of
1021 subcortical neurons. *J Neurosci* 24: 4373-81
1022 Travison TG, Araujo AB, O'Donnell AB, Kupelian V, McKinlay JB. 2007. A population-level
1023 decline in serum testosterone levels in American men. *J Clin Endocrinol Metab* 92:
1024 196-202
1025 Tuscher JJ, Szinte JS, Starrett JR, Krentzel AA, Fortress AM, et al. 2016. Inhibition of local
1026 estrogen synthesis in the hippocampus impairs hippocampal memory consolidation
1027 in ovariectomized female mice. *Horm Behav* 83: 60-67
1028 Valle A, Santandreu FM, García-Palmer FJ, Roca P, Oliver J. 2008. The serum levels of
1029 17beta-estradiol, progesterone and triiodothyronine correlate with brown adipose
1030 tissue thermogenic parameters during aging. *Cell Physiol Biochem* 22: 337-46
1031 VanGuilder HD, Farley JA, Yan H, Van Kirk CA, Mitschelen M, et al. 2011. Hippocampal
1032 dysregulation of synaptic plasticity-associated proteins with age-related cognitive
1033 decline. *Neurobiology of disease* 43: 201-12
1034 Veng LM, Granholm AC, Rose GM. 2003. Age-related sex differences in spatial learning and
1035 basal forebrain cholinergic neurons in F344 rats. *Physiology & behavior* 80: 27-36
1036 Vincent SL, Peters A, Tigges J. 1989. Effects of aging on the neurons within area 17 of rhesus
1037 monkey cerebral cortex. *The Anatomical record* 223: 329-41
1038 Vouimba RM, Foy MR, Foy JG, Thompson RF. 2000. 17beta-estradiol suppresses expression
1039 of long-term depression in aged rats. *Brain Res Bull* 53: 783-7
1040 Wagner BA, Braddick VC, Batson CG, Cullen BH, Miller LE, Spritzer MD. 2018. Effects of
1041 testosterone dose on spatial memory among castrated adult male rats.
1042 *Psychoneuroendocrinology* 89: 120-30
1043 West MJ, Coleman PD, Flood DG, Troncoso JC. 1994. Differences in the pattern of
1044 hippocampal neuronal loss in normal ageing and Alzheimer's disease. *Lancet*
1045 *(London, England)* 344: 769-72
1046 West MJ, Kawas CH, Stewart WF, Rudow GL, Troncoso JC. 2004. Hippocampal neurons in
1047 pre-clinical Alzheimer's disease. *Neurobiology of aging* 25: 1205-12
1048 Wilson IA, Ikonen S, McMahan RW, Gallagher M, Eichenbaum H, Tanila H. 2003. Place cell
1049 rigidity correlates with impaired spatial learning in aged rats. *Neurobiology of aging*
1050 24: 297-305
1051 Woodruff-Pak DS, Foy MR, Akopian GG, Lee KH, Zach J, et al. 2010. Differential effects and

rates of normal aging in cerebellum and hippocampus. *Proc Natl Acad Sci U S A* 107: 1624-9

Wu D, Lin G, Gore AC. 2009. Age-related changes in hypothalamic androgen receptor and estrogen receptor alpha in male rats. *The Journal of comparative neurology* 512: 688-701

Yamaguchi N, Yuri K. 2012. Changes in oestrogen receptor-beta mRNA expression in male rat brain with age. *Journal of neuroendocrinology* 24: 310-8

Figures

Figure 1

Male hippocampal steroid metabolism pathways, including enzymes and receptors examined in the current study. Straight arrows indicate 3m hippocampal pathways and dotted arrows indicate 24m hippocampal pathways. Relative thickness of arrow implies flow rate of metabolism.

Sufficient PROG is supplied to the hippocampus via blood PROG circulation in both 3m and 24m. Hippocampal androgen synthesis capacity from PROG to T depending on P450(17α) and 17β-HSD (1,3) decreased at 24m. Because T is rapidly and efficiently converted to DHT by 5a-reductase (highly expressed even at 24m), resultant T level may be low (~0.15 nM). T supply from circulation is very poor (~0.3 nM plasma) at 24m. However at 3m, 70% of hippocampal T (15 nM) is supplied via blood circulation (Hojo et al 2009). T is converted to E2 by P450arom, rather slowly. E2 is very stably present without degradation (Hojo et al 2009), but DHT is further converted to 5α-androstanediol by 3α-hydroxysteroid dehydrogenase (3α-HSD). Very low plasma T, DHT levels at 24m cannot contribute to hippocampal T, DHT levels. Note that plasma E2 level is already very low at 3m and 24 male.

PROG: progesterone, ADione: androstenedione, T: testosterone, DHT: dihydrotestosterone, E2: estradiol, 3α-ADiol: 3α-androstanediol.

Figure 2

Age-induced decrease of the spine density in hippocampal CA1 pyramidal neurons. Spines were analyzed along the secondary dendrites of CA1 pyramidal neurons in the stratum radiatum in 3m and 24m male rats. (A) Representative images of confocal

micrographs; the spines along dendrite in 3m (3m) and 24m (24m). Maximal intensity projection onto XY plane from z-series confocal micrographs (MAX-XY), images analyzed by Spiso-3D (Spiso), and three dimensional model illustrations (Model) are shown together. Scale bar, 5 μm. (B) The total spine density of 3m and 24m. Vertical axis represents the average number of spines per 1 μm of dendrite. Data are represented as mean ± SEM. Closed column, 3m; open column, 24m. (C) Histogram of spine head diameters in 3m (closed circle) and 24m (open circle). (D) Density of three subtypes of spines in 3m (closed column) and 24m (open column). From left to right, small-head spines (Small), middle-head spines (Middle), and large head spines (Large).
Data are represented as mean ± SEM. Statistical significance yielded $*p < 0.05$ and $**p < 0.01$.

Figure 3

Androgen (DHT and T) - induced increase of the spine density in hippocampal CA1 neurons of 24m male rat, after 17 h of androgen administration. (A) Representative images of confocal micrographs; the spines along dendrite in 24m + DHT, 24m + DHT + Flu, 24m + T, 24m + T + Flu. Maximal intensity projection onto XY plane from z-series confocal micrographs (MAX-XY), images analyzed by Spiso-3D (Spiso), and three dimensional model illustrations (Model) are shown together. Scale bar, 5 μm. (B) Comparison of the total spine density after androgen and blocker administration. (C and D) Morphology change in spines. (C1 and C2) Histogram of spine head diameters in 24m (closed square), 24m + DHT (open circle) and 24m + DHT + Flu (gray circle), and 24m (closed square), 24m + T (open circle), 24m + T + Flu (gray circle). (D1 and D2) Density of three subtypes of spines, small-head spine (Small), middle-head spine (Middle), and large-head spine (Large). From left to right of (D1), 24m (closed column), 24m + DHT (open column), 24m + DHT + Flu (gray column). From left to right of (D2), 24m (closed column), 24m + T (open column), 24m + T + Flu (gray column). Data are represented as mean ± SEM. Statistical significance yielded $*p < 0.05$ and $**p < 0.01$.

Figure 4

Age-induced decrease in T and DHT levels in the hippocampus and plasma from 3m, 12m and 24m.
The vertical axis indicates the level of DHT (A), T (B), and E2 (C). Concentrations of DHT (A), T (B), and E2 (C) in 24m and 12m hippocampus are compared with those in 3m. Data of 3m are taken from Hojo et al., (2009) (Hojo et al 2009). DHT-picolinoyl

(m/z = 203), T-picolinoyl (m/z = 253), and E2-PFBz-picolinoyl (m/z = 339) are analyzed by using LC-MS/MS as described in earlier studies (Hojo et al 2009). Data are represented as mean ± SEM. Statistical significance yielded *$p < 0.05$ and **$p < 0.01$ vs 3m hippocampus group, and $^{\#\#}$ $p < 0.01$ vs 3m plasma group.

Figure 5

Age-induced change of steroidogenic enzymes, cholesterol transport proteins and steroid receptors in the hippocampus.

Upper panels show representative PCR images visualized with ethidium bromide (EtBr) staining. From left to right, 100 bp DNA ladder (M), 3m, 12m, 24m, and the sample without template cDNA as negative control (Nc).

Lower panels show mRNA expression levels of the (A) *Gapdh*, (B-K) steroidogenic enzymes ((B) *Cyp17a1*, (C) *Hsd17b1*, (D) *Hsd17b3*, (E) *Srd5a1*, (F) *Srd5a2*, (G) *Cyp19a1*, (H) *Star*, (I) *Tspo*, (J) *Cyp11a1*, (K) *3β-HSDI*), and (L-O) steroid receptors ((L) *Ar*, (M) *Esr1*,(N) *Esr2* and (O) *Pgr*) in 3m, 12m and 24m rats. The vertical axis indicates the relative expression level for each mRNA calculated from the intensity of EtBr bands. (A) The *Gapdh* mRNA expression level was normalized with 3m which is set to be 100%. (B-O) The mRNAs expression levels of each steroidogenic enzymes (B-G, J and K), cholesterol transport proteins (H and I) and steroid receptors (L-O) were normalized with *Gapdh* and the corresponding mRNA expression in 3m rats, as described in Methods. Each value is mean ± SEM. Statistical significance yielded *$p < 0.05$, **$p < 0.01$, ***$p < 0.001$. Data are taken from duplicate determinations of 4 rats at each age.

Figure 6

Comprehensive comparison of expression levels of mRNAs between different enzymes and receptors in (A) 24m, (B) 12m and (C) 3m brains. The comparison was performed using the method as described in Materials and Methods. The normalization of each mRNA was performed by setting *Cyp19a1* of 3m Hi as 100%. Data are also normalized by *Gapdh*. The vertical scale is different for each enzymes/receptors. For comparison, the vertical scale should amplify by100-fold for *Srd5a1*; by 50-fold for *Ar*; by10-fold for *Hsd17b1* and *Esr1*; by1-fold for *Cyp17a1*, *Hsd17b3*, *Srd5a2*, *Cyp19a1* and *Esr2*. The data of 3m was modified from Kimoto *et al*. (Kimoto et al 2010).

Figure 1

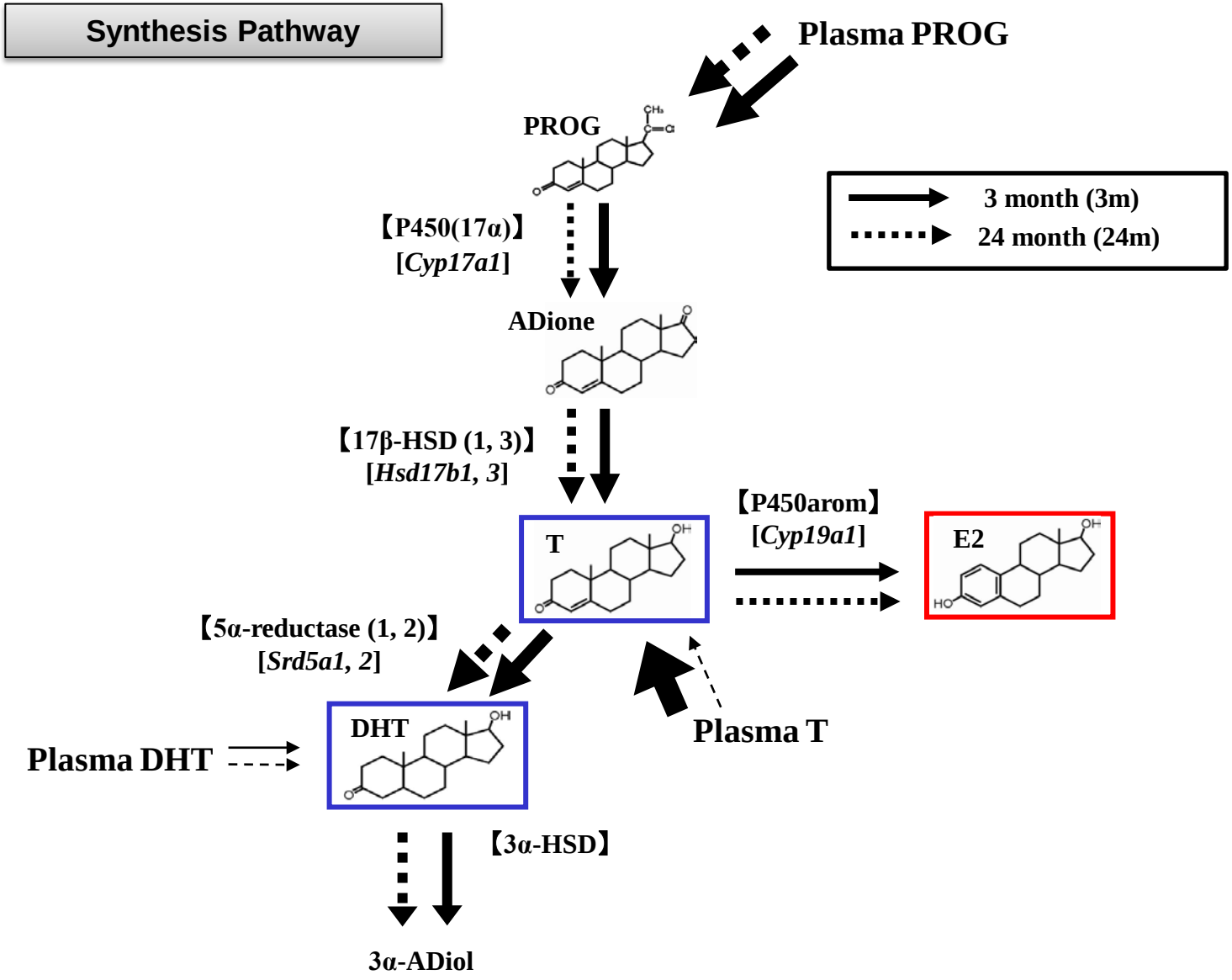
Synthesis Pathway
Plasma PROG
PROG
【P450(17α)】
[*Cyp17a1*]
3 month (3m)
24 month (24m)
ADione
【17β-HSD (1, 3)】
[*Hsd17b1, 3*]
T
【P450arom】
[*Cyp19a1*]
E2
【5α-reductase (1, 2)】
[*Srd5a1, 2*]
DHT
Plasma T
Plasma DHT
【3α-HSD】
3α-ADiol

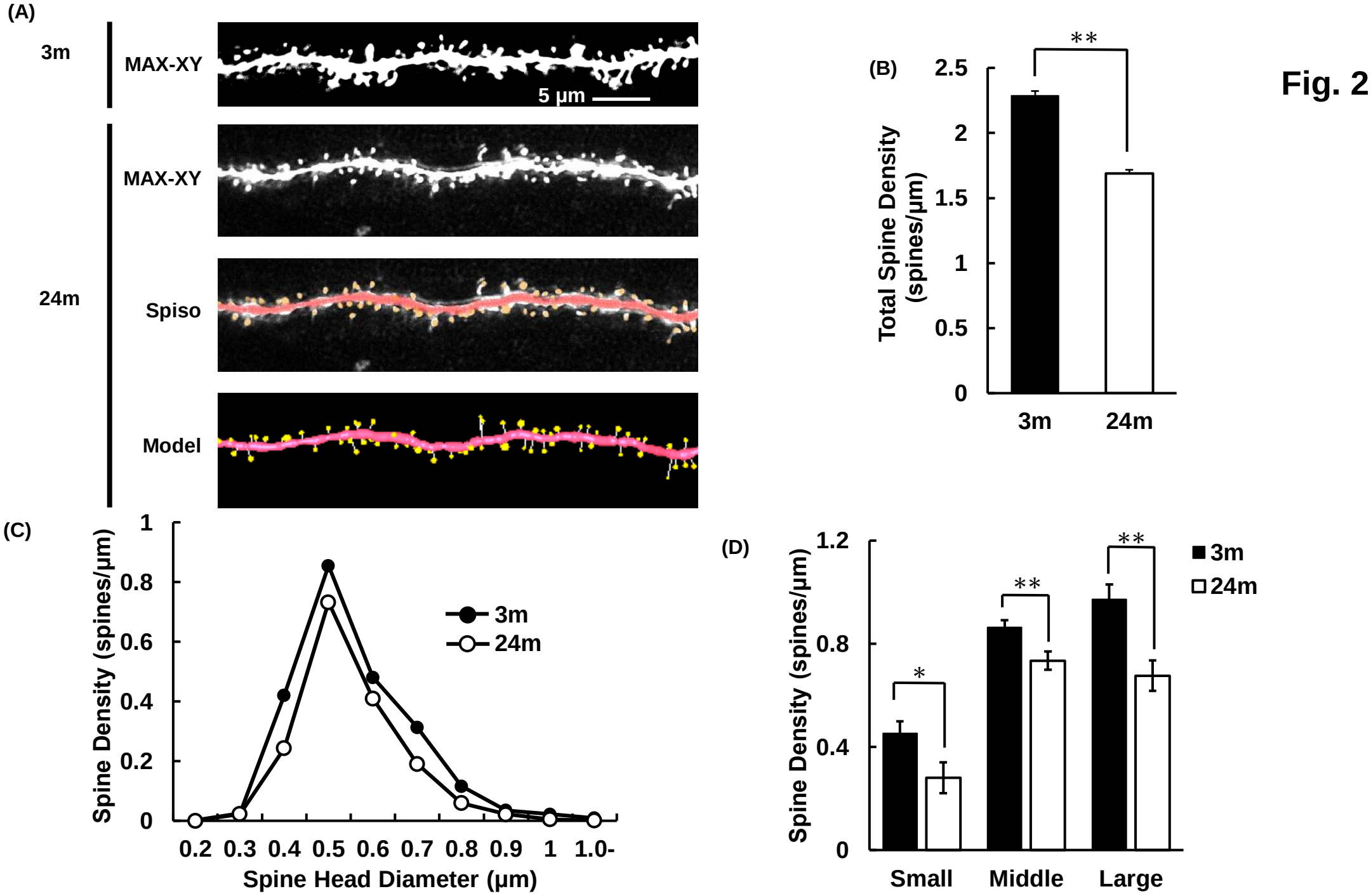
(A)
3m
MAX-XY
5 μm
24m
MAX-XY
Spiso
Model
(B)
Total Spine Density (spines/μm)
2.5
2
1.5
1
0.5
0
**
3m
24m
(C)
Spine Density (spines/μm)
1
0.8
0.6
0.4
0.2
0
3m
24m
0.2 0.3 0.4 0.5 0.6 0.7 0.8 0.9 1 1.0-
Spine Head Diameter (μm)
(D)
Spine Density (spines/μm)
1.2
0.8
0.4
0
*
**
**
3m
24m
Small
Middle
Large

Fig. 2

Fig. 3A

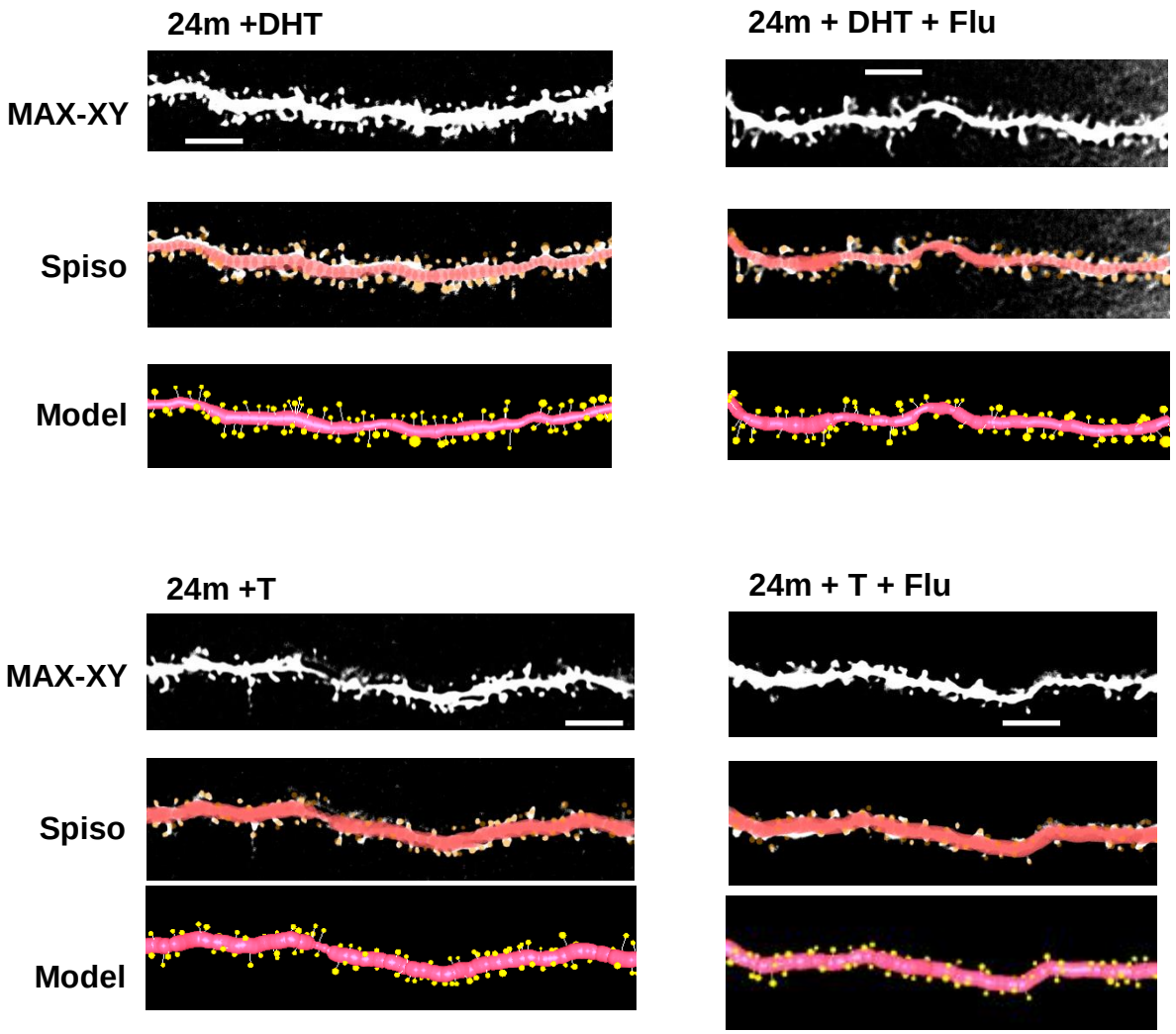
24m +DHT
24m + DHT + Flu
MAX-XY
Spiso
Model
24m +T
24m + T + Flu
MAX-XY
Spiso
Model

Fig. 3B

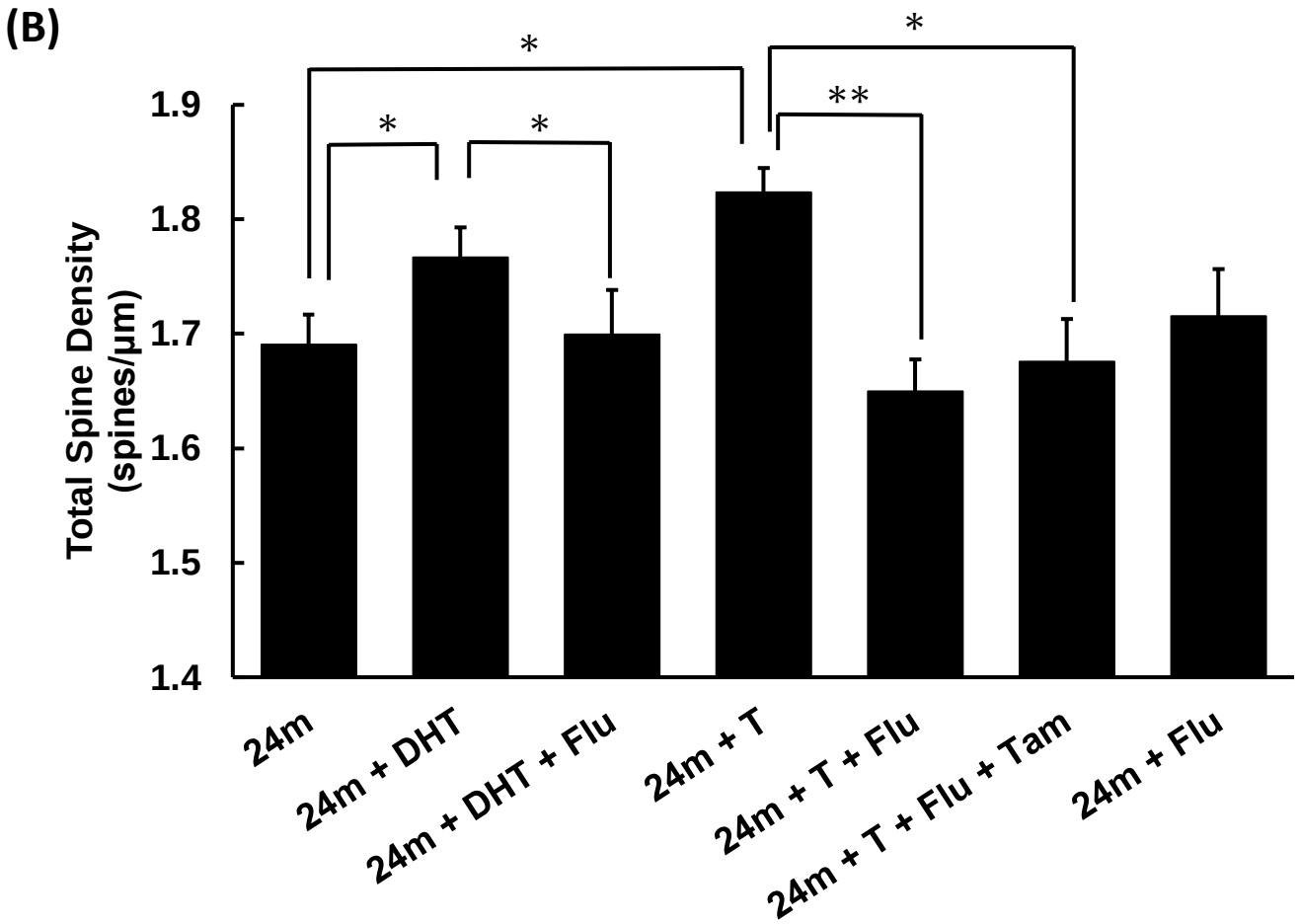
(B)
Total Spine Density
(spines/µm)
1.9
1.8
1.7
1.6
1.5
1.4
*
*
*
*
**
24m
24m + DHT
24m + DHT + Flu
24m + T
24m + T + Flu
24m + T + Flu + Tam
24m + Flu

Fig. 3C, 3D

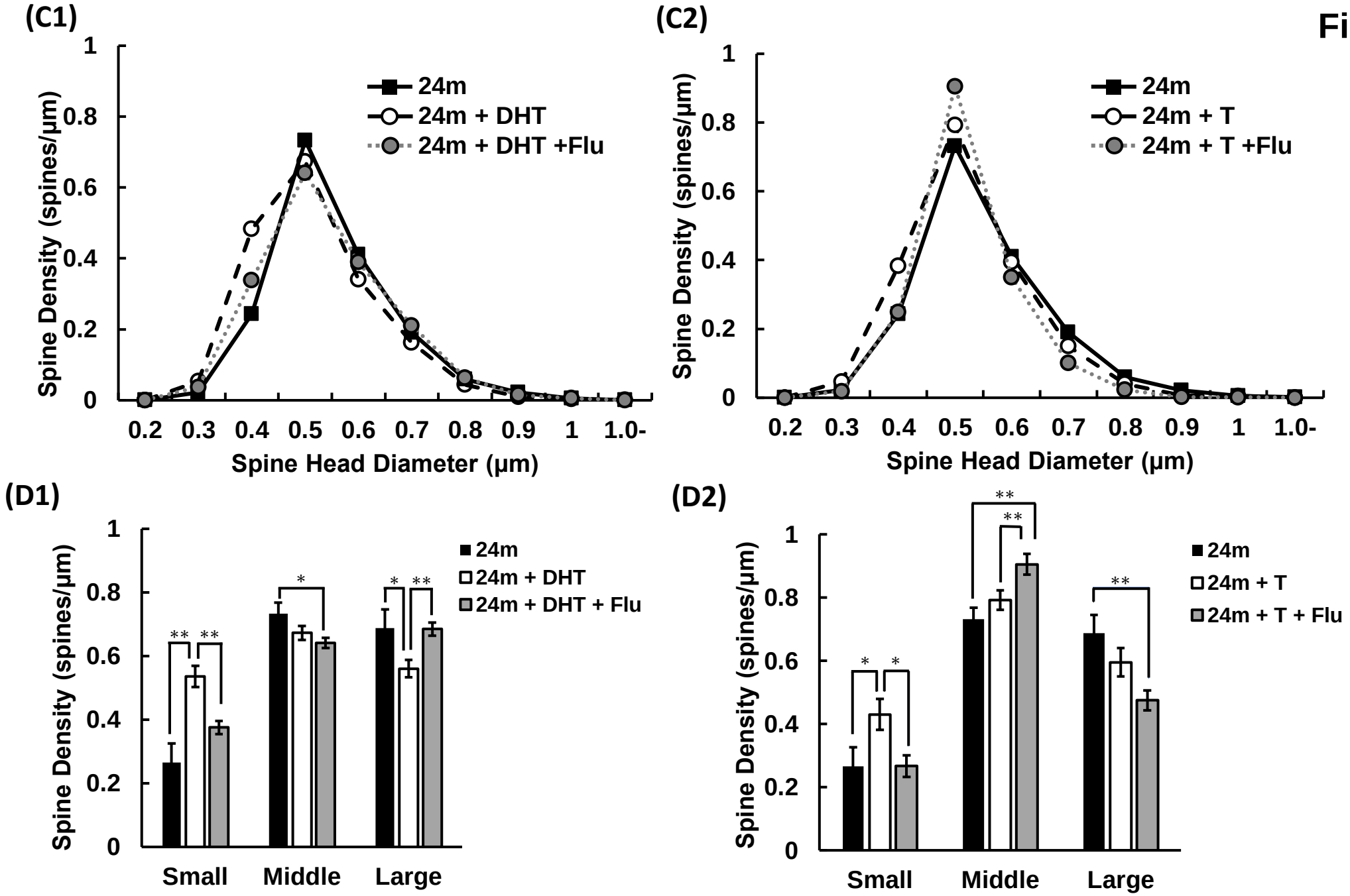
(C1)
Spine Density (spines/μm)
Spine Head Diameter (μm)
24m
24m + DHT
24m + DHT +Flu
(C2)
24m
24m + T
24m + T +Flu
(D1)
24m
24m + DHT
24m + DHT + Flu
Small
Middle
Large
(D2)
24m
24m + T
24m + T + Flu

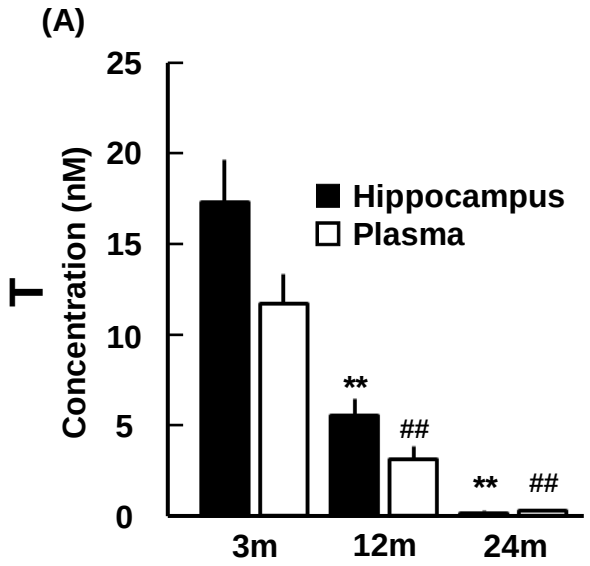
(A)
T
Concentration (nM)
25
20
15
10
5
0
Hippocampus
Plasma
**
##
**
##
3m
12m
24m

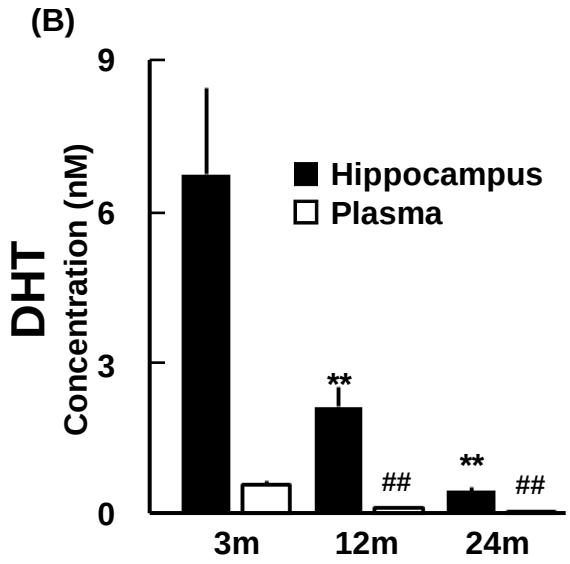
(B)
DHT
Concentration (nM)
9
6
3
0
Hippocampus
Plasma
**
##
**
##
3m
12m
24m

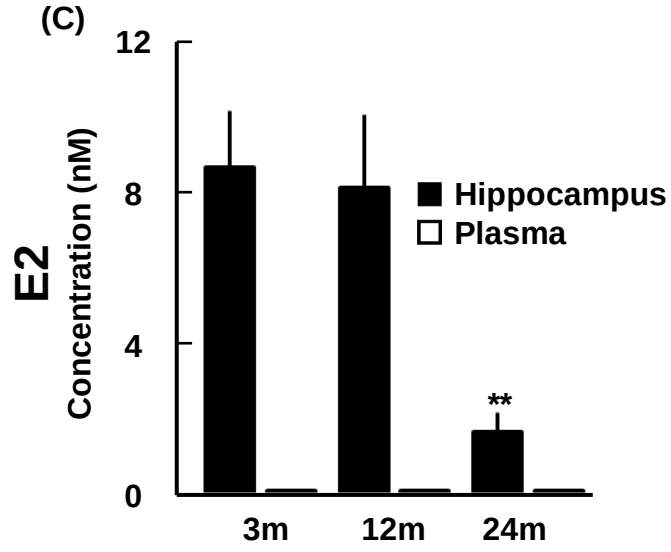
(C)
E2
Concentration (nM)
12
8
4
0
Hippocampus
Plasma
**
3m
12m
24m

Fig. 4

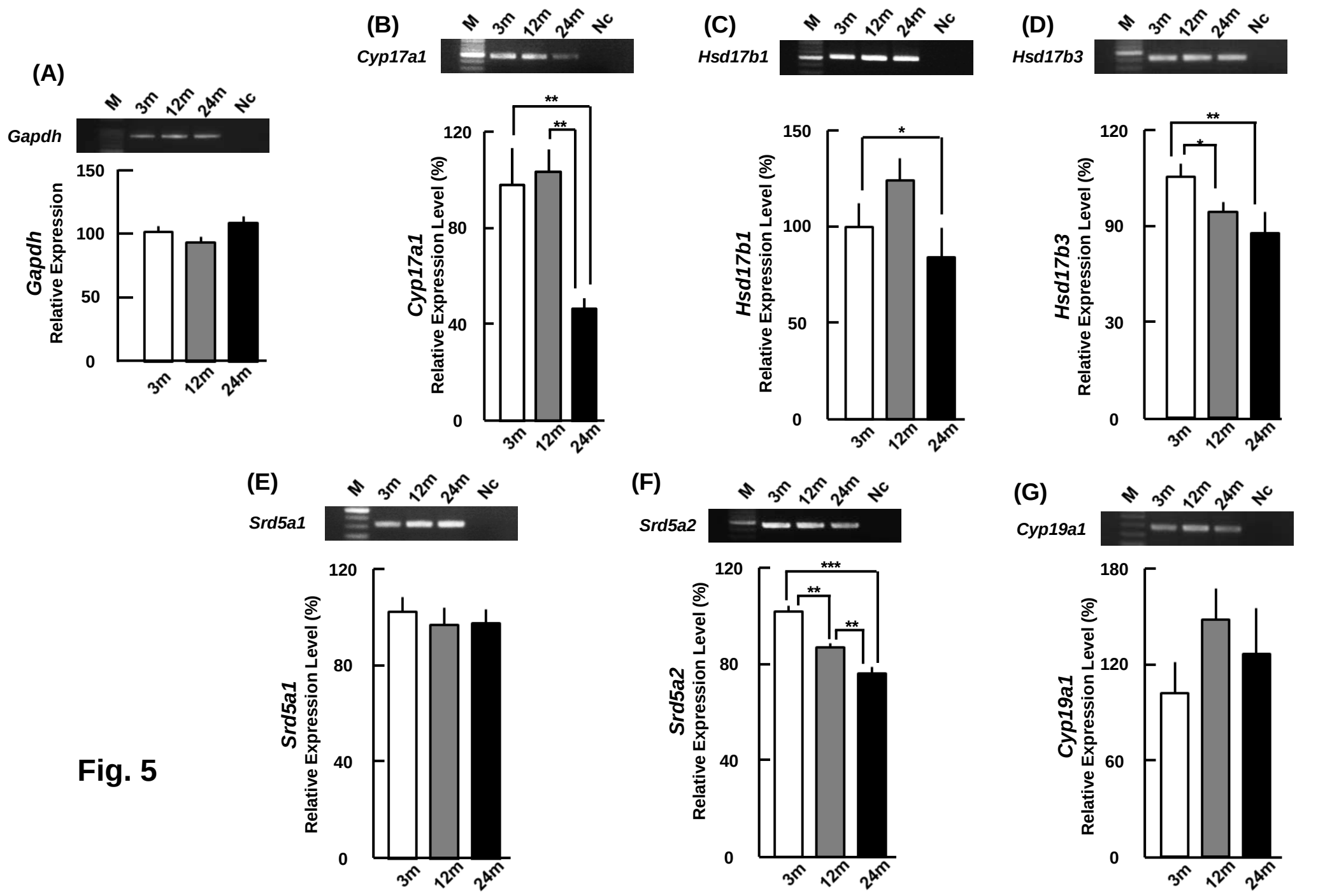
(A)
M
3m
12m
24m
Nc
Gapdh
Gapdh
Relative Expression
150
100
50
0
3m
12m
24m
(B)
Cyp17a1
Cyp17a1
Relative Expression Level (%)
120
80
40
0
**
**
(C)
Hsd17b1
Hsd17b1
Relative Expression Level (%)
150
100
50
0
*
(D)
Hsd17b3
Hsd17b3
Relative Expression Level (%)
120
90
30
0
**
*
(E)
Srd5a1
Srd5a1
Relative Expression Level (%)
120
80
40
0
(F)
Srd5a2
Srd5a2
Relative Expression Level (%)
120
80
40
0
***
**
**
(G)
Cyp19a1
Cyp19a1
Relative Expression Level (%)
180
120
60
0

Fig. 5

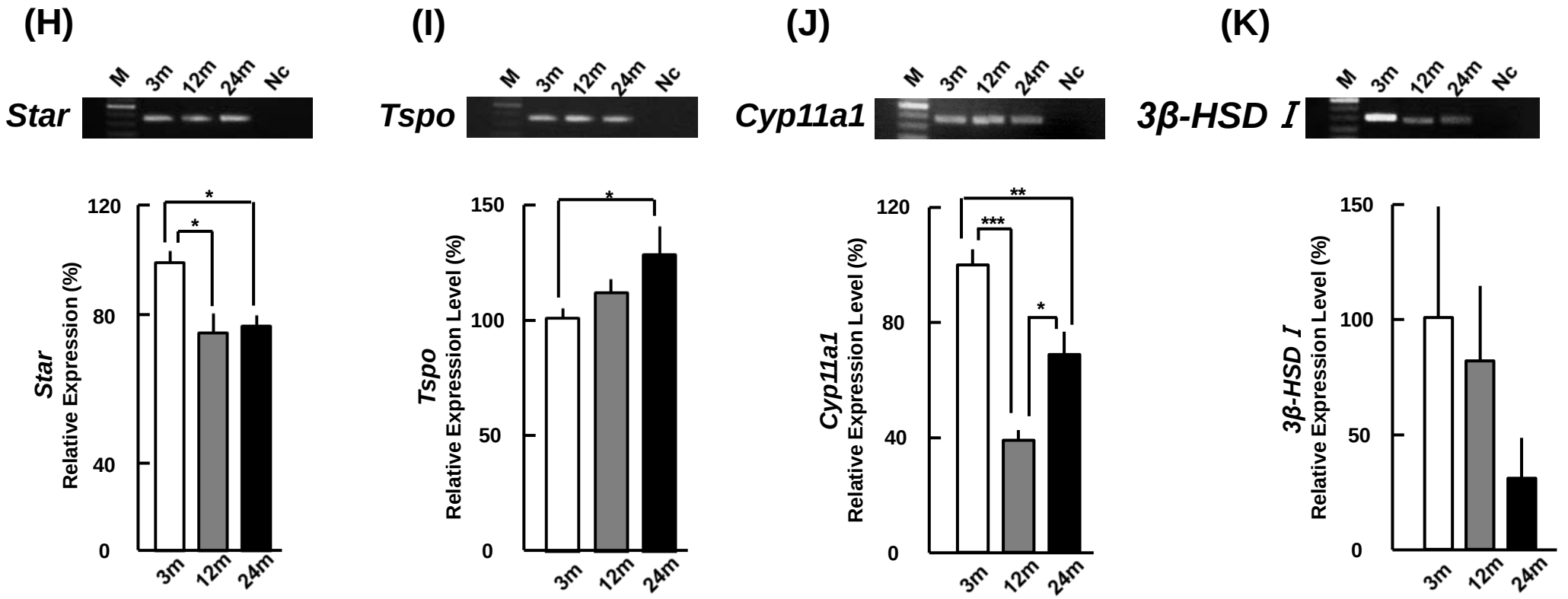
(H)
(I)
(J)
(K)
Star
Tspo
Cyp11a1
3β-HSD I
M
3m
12m
24m
Nc
Relative Expression (%)
Relative Expression Level (%)
0
40
80
120
50
100
150
*
**
***

Fig. 5

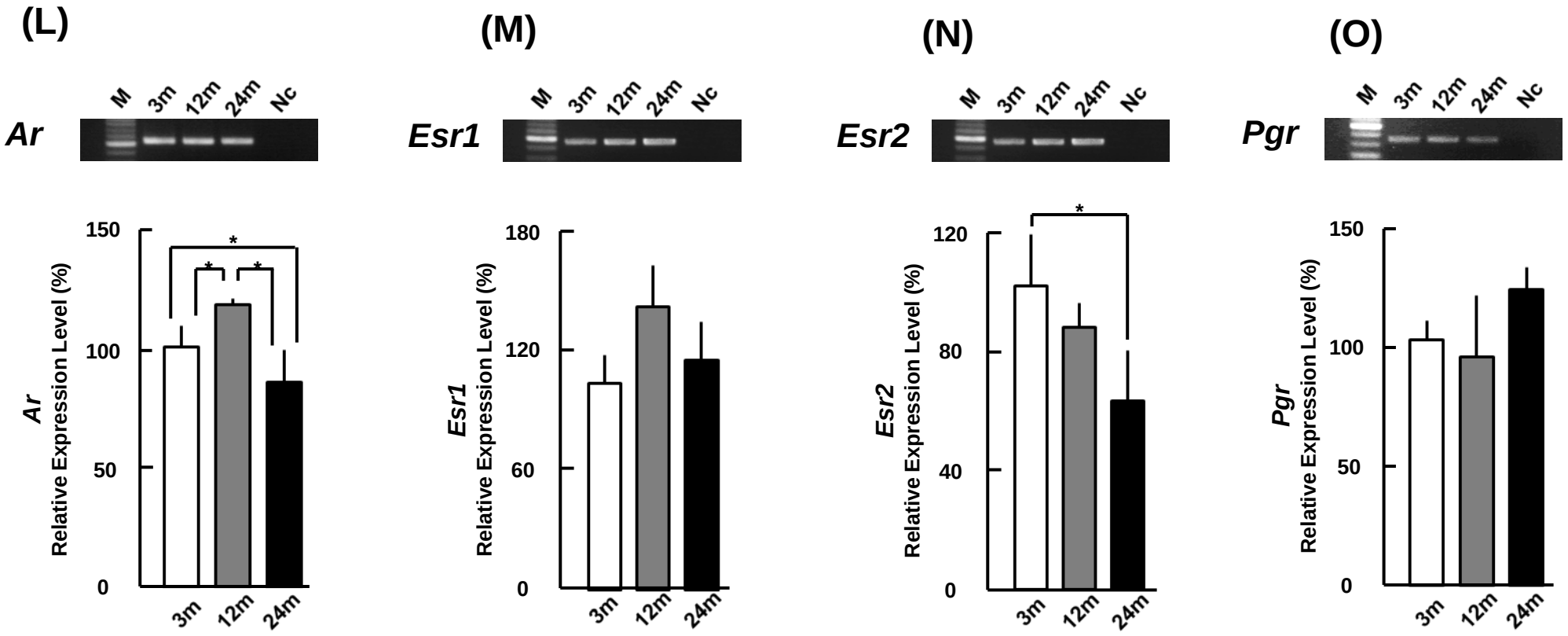
(L)
(M)
(N)
(O)
Ar
Esr1
Esr2
Pgr
M
3m
12m
24m
Nc
Relative Expression Level (%)
150
100
50
0
180
120
60
80
40
*

Fig. 5

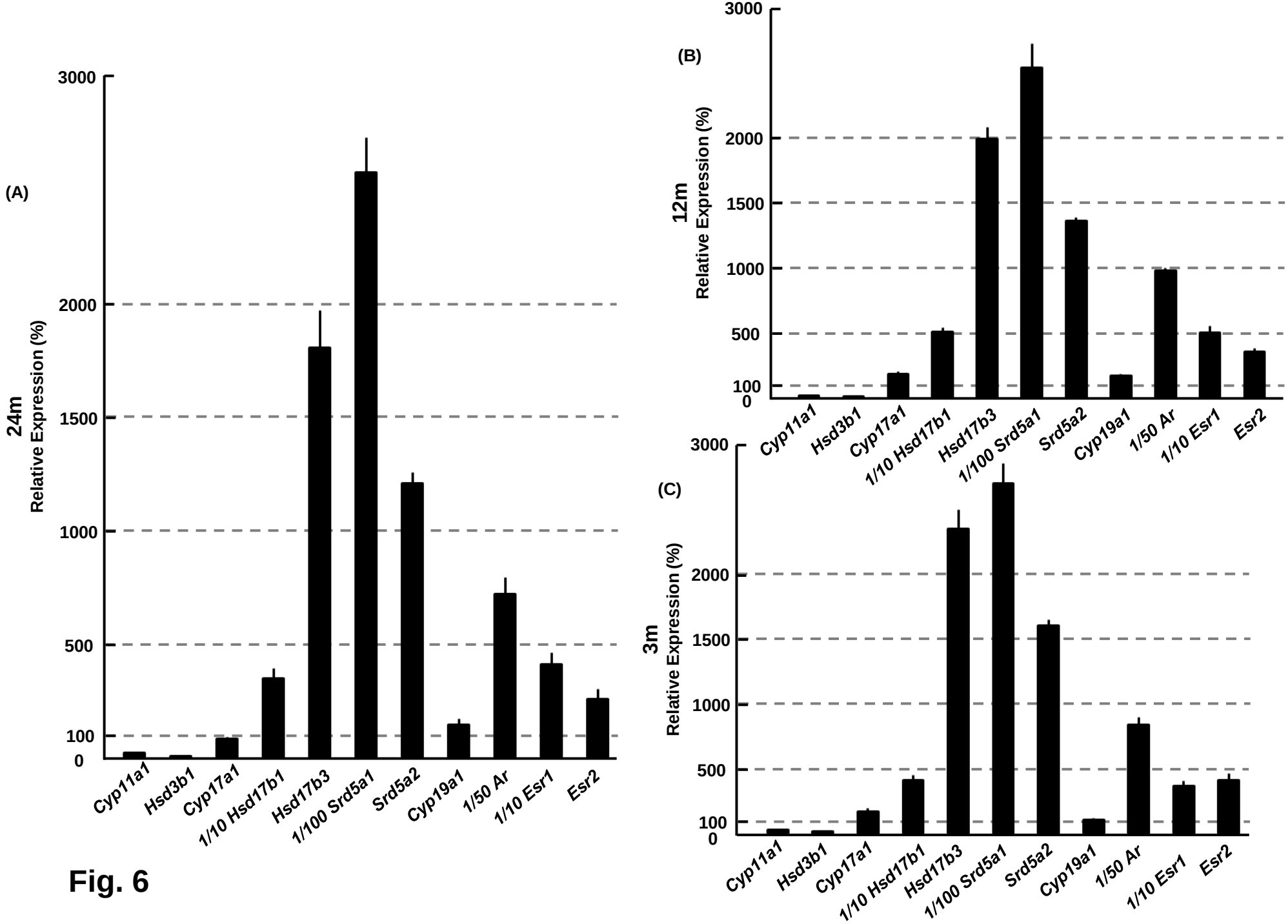
(A)
24m
Relative Expression (%)
3000
2000
1500
1000
500
100
0
Cyp11a1
Hsd3b1
Cyp17a1
1/10 Hsd17b1
Hsd17b3
1/100 Srd5a1
Srd5a2
Cyp19a1
1/50 Ar
1/10 Esr1
Esr2
(B)
12m
Relative Expression (%)
3000
2000
1500
1000
500
100
0
Cyp11a1
Hsd3b1
Cyp17a1
1/10 Hsd17b1
Hsd17b3
1/100 Srd5a1
Srd5a2
Cyp19a1
1/50 Ar
1/10 Esr1
Esr2
(C)
3m
Relative Expression (%)
3000
2000
1500
1000
500
100
0
Cyp11a1
Hsd3b1
Cyp17a1
1/10 Hsd17b1
Hsd17b3
1/100 Srd5a1
Srd5a2
Cyp19a1
1/50 Ar
1/10 Esr1
Esr2

Fig. 6

5. Supplementary materials

5.1 Supplementary methods

Mass-spectrometric assay of steroids

For assay of hippocampal E2 concentration, freshly prepared hippocampus (but not frozen-thawed hippocampus) must be used (Kawato et al 2025). We here explain the reason. The freeze-thaw processes using deep freezer (-80 degree) may damage brain tissues and cells due to crystallization of intercellular water (in freezing processes) and melting of intercellular ice (in thawing processes). Crystallization of intercellular water by freezing may break cell membranes, leading to leaking and losing of antioxidants (such as glutathione and vitamin C) and antioxidant enzymes (such as superoxide dismutase and glutathione peroxidase). Reactive oxygen species produced from mitochondria may easily attack lipids in cell membranes in the absence of these antioxidants and antioxidant enzymes. Melting of intercellular ices may also break cell membranes, leading to leaking and losing of antioxidants and antioxidant enzymes. Under these bad conditions, membrane lipid peroxidation would occur, leading to oxidation of OH at C-3 position of E2, resulting in modification of E2 molecules. Resultant E2 concentration may become 0.05 - 0.1 nM in adult male rats (Kawato et al 2025). In this way, the hippocampal E2 concentration may significantly decrease in frozen-thawed hippocampal tissues.

In this way, using freshly prepared (but not frozen-thawed) hippocampal tissues, we can always observed the E2 concentration higher than 3 nM in adult 3m male rats (Hojo et al 2009), (Kato et al 2013).

Interestingly and surprisingly, hippocampal T concentration was not considerably different between frozen-thawed hippocampus and freshly prepared hippocampus (Kawato et al 2025). This is because, T has an oxygen (O) at C-3 position which is resistant to oxidation and inactivation. Therefore, T molecules might not be modified by freeze-thaw processes of hippocampal tissues.

5.2 Supplementary Results

Immunostaining of hippocampal enzymes and receptors (Fig. S3)

In 24m rats, cytochrome P450(17α) and cytochrome P450arom were expressed in pyramidal neurons of CA1-CA3 and granule cells in dentate gyrus (DG) (Fig. S3). The

distributions of these enzyme were similar to those obtained in 3m rats (Kawato et al 2002) (Hojo et al 2004) . The stained intensity of P450(17α) and P450arom was not significantly changed between 24m and 3m (Hojo et al 2004). On the other hand, the stained intensity of P450scc at 24m was dramatically weaker than that in 3m (Kimoto et al 2001). The stained intensity of PSD95, synaptic marker protein, very weak at 24m, which is a good agreement with earlier reports (Fig. S3) (VanGuilder et al 2010). Since immunostaining intensity does not have enough sensitivity, almost no significant changes were observed in the expression levels of sex-steroid receptors (AR and ERα) between 24m and 3m (Fig. S3) (Mukai et al 2007). In 24m hippocampal slices, ERα was expressed with almost the same level in pyramidal neurons of CA1-CA3 regions and granule cell in DG, however, AR expression level was the strongest in CA1, and almost no expression in DG (Hojo et al 2014).

It should be noted that the quantitativity of expression levels from immunostaining analysis is low, therefore, less than ~30% change in expression level cannot be evaluated with immunostaining data.

5. 3 Supplementary Discussion

5.3.1 Age-dependent changes of AR, ER and steroidogenic enzymes in non-hippocampal brain regions

Age-dependent changes of steroid receptors and steroidogenic enzymes showed very different tendency in different brain regions, including the hippocampus, Hy, CC and CL in rats.

Hy has the highest expressions of steroid receptors (AR and ER) and steroidogenic enzymes among other regions (hippocampus, Hy, CC and CL), and often they showed no decline with Hy aging (Munetomo et al 2015).

With aging of Hy, mRNAs of AR and ERα increased, and mRNA of ERβ, P450arom and 5α-reductase did not decrease by going from 3m to 24m (Munetomo et al 2015). In Hy, the number of ERα–immunoreactive cells and AR-immunoreactive cells increased with age (Wu et al 2009).

Since the sealing of blood-brain-barrier in Hy is much looser than that in other brain regions, including hippocampus, CC and CL, the decline in plasma sex steroids may induce resistance against the tendency of age-induced decrease in receptors and steroidogenic enzymes in Hy. These age-resistant phenomena might occur, through hypothalamus-pituitary-gonadal axis during aging processes, due to strong interactions

between plasma sex-steroids and Hy.

The expression levels of ERα mRNA increased in CC from 3m to 24m, but did not significantly change in CL as similar to the hippocampus (Munetomo et al 2015).

On the other hand, AR mRNA level decreased in CC at 24m, but did not change in CL with age (Munetomo et al 2015).

With aging, the expression level of ERβ mRNA did not change in CC, but decreased in CL (Munetomo et al 2015). ERβ mRNA-positive cells, however, decreased in CC layer 6 and amygdala (Yamaguchi & Yuri 2012).

Interestingly, in CC and CL, almost no expression of P450arom mRNA was observed over 3m − 24m (Kimoto et al 2010) (Munetomo et al 2015), implying that the activity of estrogen synthesis in CC and CL would be very weak.

CC and CL of young adult and aged rats might need E2 supply from other regions, including Hy or hippocampus, via diffusion/penetration of E2 through cerebrospinal fluid, since hippocampus and Hy could have relatively high activity of E2 synthesis (Hojo et al 2009) (Kimoto et al 2010). Penetration of low level E2 (~ 0.02 nM) from blood plasma may not be sufficient in the adult and aged male brain. On the other hand, E2 may be sufficiently present in CL in neonatal stage, since *Cyp19a1* is significantly expressed in CL at neonatal stage (Sakamoto et al 2003). Note that the expression level of P450arom mRNA in Hy is approxi. 2-fold of that in the hippocampus and did not decrease with age (Munetomo et al 2015).

5.3.2 Difference in hippocampal T levels between rat and human in old age

The reason why the level of T in the hippocampus and plasma decreased to extremely low level at 24m (Fig. 3) may be due to extremely poor adrenal-synthesized DHEA in rats, because of lacking cytochrome P450(17α) in the adrenal glands. (Le Goascogne et al 1991). Aging induced impairment of DHEA and T synthesis within rat testis directly decreases T levels of the plasma and the hippocampus, because 70 – 80% hippocampal T is derived from the blood circulation (Hojo et al 2009).

On the other hand, human adrenals can produce high level of DHEA because of sufficient expression of adrenal cytochrome P450(17α). This DHEA would be converted to T in other peripheral organs. Therefore, human plasma T did not decrease extremely, but moderately decreased along with aging (Travison et al 2007). Difference in aged T effects on rodents and human should be carefully considered.

6. Supplementary Figures

Supplementary Figure S1

Steroid derivatives and their fragmented ions used for analysis with LC-MS/MS. (A) E2-3-pentafluorobenzoxy-17-picolinoyl-ester (m/z = 558) and its fragmented ion (m/z = 339), (B) T-17-picolinoyl-ester (m/z = 394) and its fragmented ion (m/z = 253), (C) DHT-17-picolinoyl-ster (m/z = 396) and its fragmented ion (m/z = 203). (D, E) Chromatographic profiles showing the retention time of the fragmented ions of E2-PFBz-picolinoyl, T-picolinoyl and DHT-picolinoyl, with the m/z transition, from 558 to 339 for E2-PFBz-picolinoyl, from 394 to 253 for T-picolinoyl, from 396 to 203 for DHT-picolinoyl, respectively. For these steroids, the retention time of the hippocampal steroid peak (D) was the same as that of standard steroid-picolinoyl (E). (E, F, G) Calibration curves for LC-MS/MS using standard steroids dissolved in ethanol. Horizontal (x) axis indicates the concentration of added standard steroid. Vertical (y) axis indicates the relative intensity obtained from the chromatogram. (A) Calibration curve for E2. Linearity was observed between 0.1 pg/mL to 1000 pg/mL (in this figure only until 400 pg/mL is shown). (B) Calibration curve for T. Linearity was observed between 0.5 pg/mL to 1000 pg/mL. (C) Calibration curve for DHT. Linearity was observed between 0.5 pg/mL to 1000 pg/mL.

Supplementary Figure S2

The expression levels of the neurotrophic factors (*Bdnf* and *Brain-Insulin1*), and senescence marker genes (*Sirt1* and *Tp53*) in the hippocampus.

Upper panels show typical PCR images. From left to right, 100 bp DNA ladder (M), 3m, 12m, 24m, and the sample without template cDNA as negative control (Nc).

Lower panels show mRNA expression levels of (A) *Bdnf* and (B) *Brain-Insulin1*, and (C) *Sirt1* and (D) *Tp53* at 3m, 12m and 24m. The vertical axis indicates the expression level for each mRNAs calculated from the intensity of EtBr bands. Each value is mean ± SEM. Statistical significance, *$p < 0.05$, **$p < 0.01$, ***$p < 0.001$. Data are taken from duplicate determinations for 4 rats at each age. The normalization of each mRNAs was performed in the same manner as Fig. 4.

Supplementary Figure S3

Immunostaining of sex steroidogenic enzymes and receptors in the 24m hippocampal slices. Moderate expressions of StAR, P450(17α), P450arom, ERα, AR are shown in CA1, CA3 and DG regions. AR is mainly expressed in CA1. In contrast,

negligible expressions of P450scc and PSD95 are shown. Scale bar 500 μm.

References

Hojo Y, Hattori TA, Enami T, Furukawa A, Suzuki K, et al. 2004. Adult male rat hippocampus synthesizes estradiol from pregnenolone by cytochromes P45017alpha and P450 aromatase localized in neurons. *Proc Natl Acad Sci U S A* 101: 865-70

Hojo Y, Higo S, Ishii H, Ooishi Y, Mukai H, et al. 2009. Comparison between hippocampus-synthesized and circulation-derived sex steroids in the hippocampus. *Endocrinology* 150: 5106-12

Hojo Y, Okamoto M, Kato A, Higo S, Sakai F, et al. 2014. Neurosteroid synthesis in adult female rat hippocampus, including androgens and allopregnanolone. *J Steroids and Hormonal Sci*: Article S4

Kato A, Hojo Y, Higo S, Komatsuzaki Y, Murakami G, et al. 2013. Female hippocampal estrogens have a significant correlation with cyclic fluctuation of hippocampal spines. *Front Neural Circuits* 7: 149

Kawato S, Hojo Y, Kimoto T. 2002. Histological and metabolism analysis of P450 expression in the brain. *Methods Enzymol* 357: 241-9

Kawato S, Ogiue-Ikeda M, Soma M, Horie S, Saito M, Minato K. 2025. Rethinking synthesis and function of neuro-estrogen and neuro-androgen in the hippocampus: some methodological problems and possible solutions. *bioRxiv*

Kimoto T, Ishii H, Higo S, Hojo Y, Kawato S. 2010. Semicomprehensive analysis of the postnatal age-related changes in the mRNA expression of sex steroidogenic enzymes and sex steroid receptors in the male rat hippocampus. *Endocrinology* 151: 5795-806

Kimoto T, Tsurugizawa T, Ohta Y, Makino J, Tamura H, et al. 2001. Neurosteroid synthesis by cytochrome p450-containing systems localized in the rat brain hippocampal neurons: N-methyl-D-aspartate and calcium-dependent synthesis. *Endocrinology* 142: 3578-89

Le Goascogne C, Sananes N, Gouezou M, Takemori S, Kominami S, et al. 1991. Immunoreactive cytochrome P-450(17 alpha) in rat and guinea-pig gonads, adrenal glands and brain. *J Reprod Fertil* 93: 609-22

Mukai H, Tsurugizawa T, Murakami G, Kominami S, Ishii H, et al. 2007. Rapid modulation

of long-term depression and spinogenesis via synaptic estrogen receptors in hippocampal principal neurons. *J Neurochem* 100: 950-67

Munetomo A, Hojo Y, Higo S, Kato A, Yoshida K, et al. 2015. Aging-induced changes in sex-steroidogenic enzymes and sex-steroid receptors in the cortex, hypothalamus and cerebellum. *The journal of physiological sciences : JPS* 65: 253-63

Sakamoto H, Mezaki Y, Shikimi H, Ukena K, Tsutsui K. 2003. Dendritic growth and spine formation in response to estrogen in the developing Purkinje cell. *Endocrinology* 144: 4466-77

Travison TG, Araujo AB, O'Donnell AB, Kupelian V, McKinlay JB. 2007. A population-level decline in serum testosterone levels in American men. *J Clin Endocrinol Metab* 92: 196-202

VanGuilder HD, Yan H, Farley JA, Sonntag WE, Freeman WM. 2010. Aging alters the expression of neurotransmission-regulating proteins in the hippocampal synaptoproteome. *J Neurochem* 113: 1577-88

Wu D, Lin G, Gore AC. 2009. Age-related changes in hypothalamic androgen receptor and estrogen receptor alpha in male rats. *The Journal of comparative neurology* 512: 688-701

Yamaguchi N, Yuri K. 2012. Changes in oestrogen receptor-beta mRNA expression in male rat brain with age. *Journal of neuroendocrinology* 24: 310-8

Fig. S1

(A)

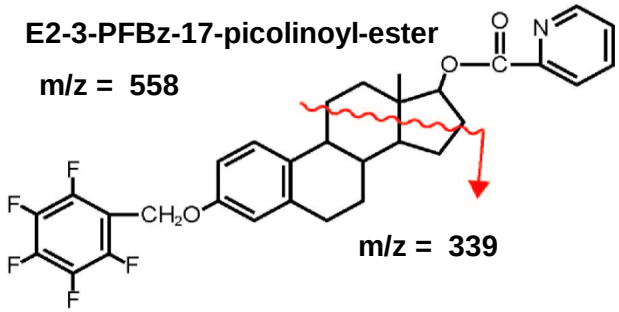
E2-3-PFBz-17-picolinoyl-ester
m/z = 558
m/z = 339

(B)

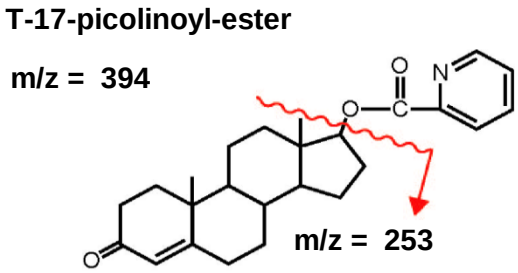
T-17-picolinoyl-ester
m/z = 394
m/z = 253

(C)

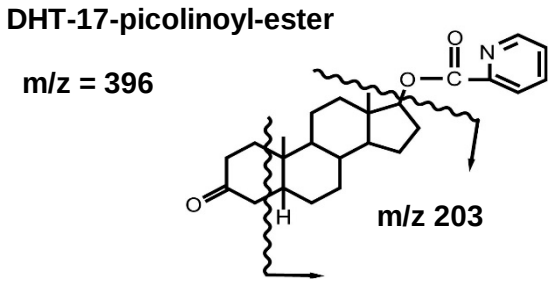
DHT-17-picolinoyl-ester
m/z = 396
m/z 203

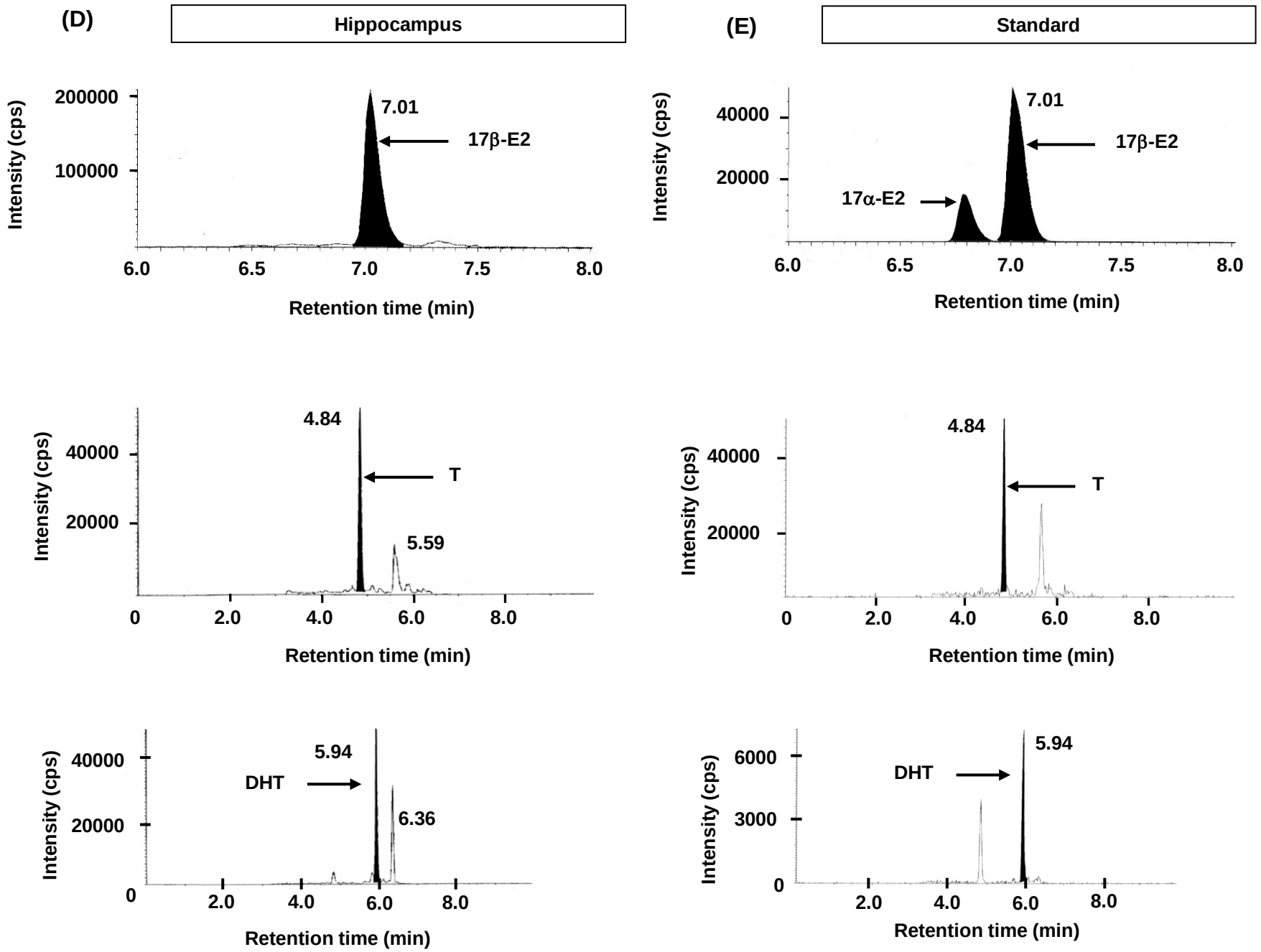
(D)
Hippocampus
(E)
Standard
Intensity (cps)
200000
100000
7.01
17β-E2
6.0
6.5
7.0
7.5
8.0
Retention time (min)
40000
20000
17α-E2
4.84
T
5.59
0
2.0
4.0
6.0
8.0
5.94
DHT
6.36
6000
3000

Fig. S1

Fig. S2

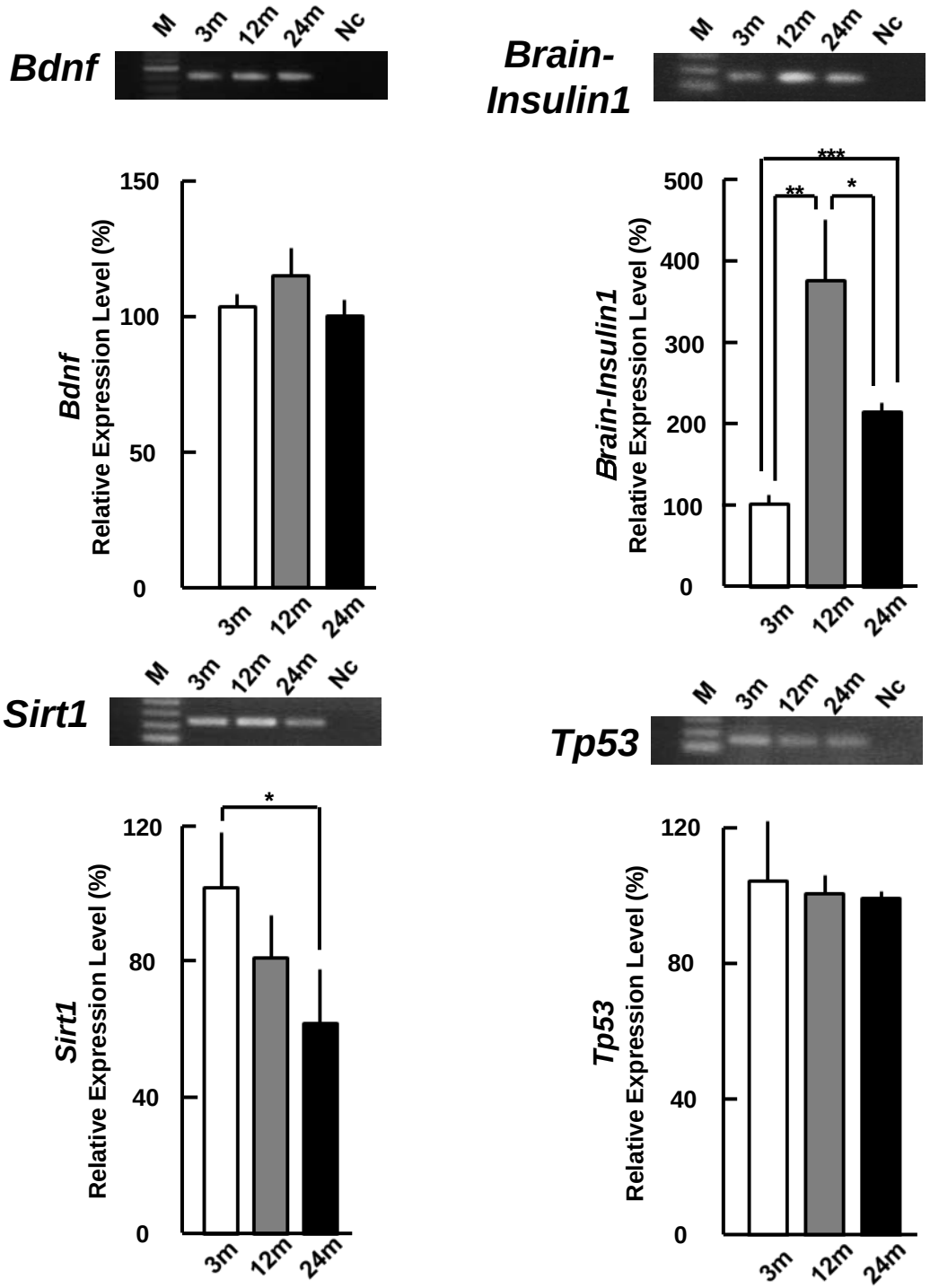
Bdnf
M
3m
12m
24m
Nc
Brain-Insulin1
Bdnf
Relative Expression Level (%)
150
100
50
0
3m
12m
24m
Brain-Insulin1
Relative Expression Level (%)
500
400
300
200
100
0
***
**
*
Sirt1
Tp53
Sirt1
Relative Expression Level (%)
120
80
40
0
*
Tp53
Relative Expression Level (%)

Fig. S3

StAR

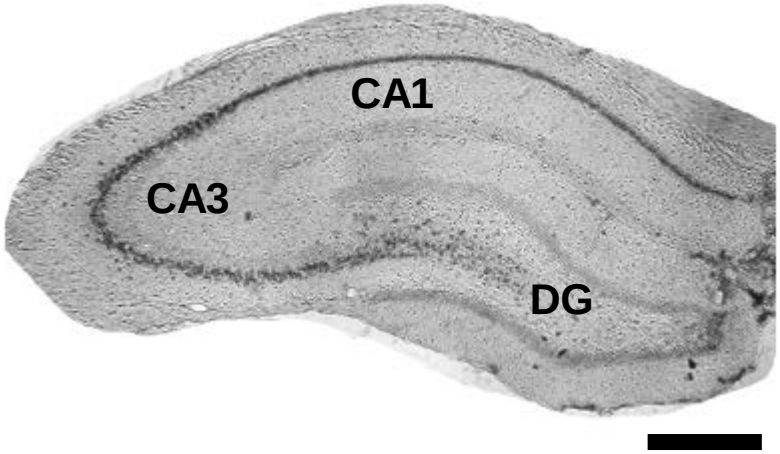

P450scc

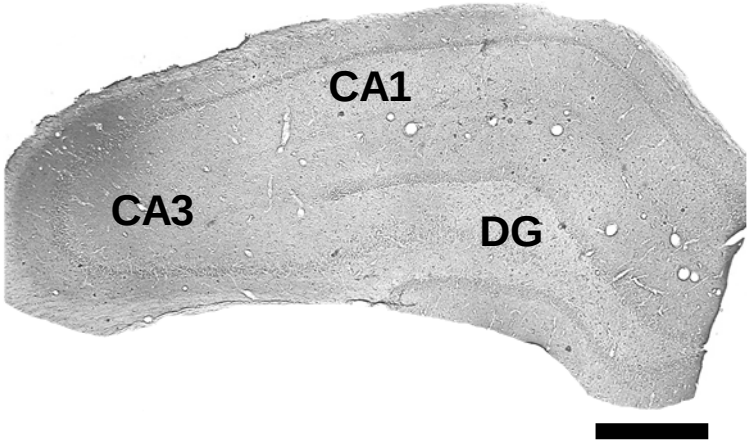

P450(17α)

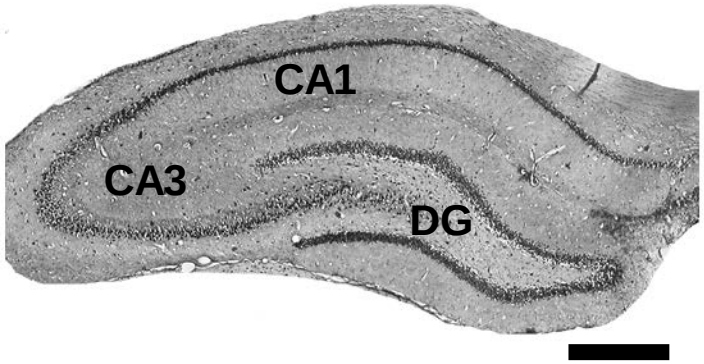

P450arom

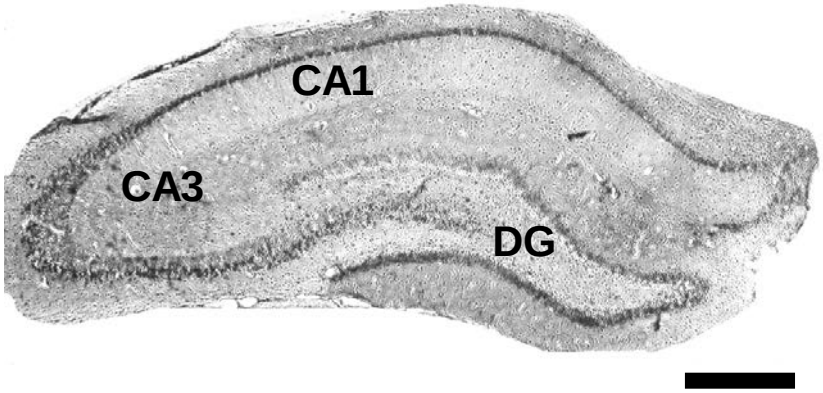

Fig. S3

ERα

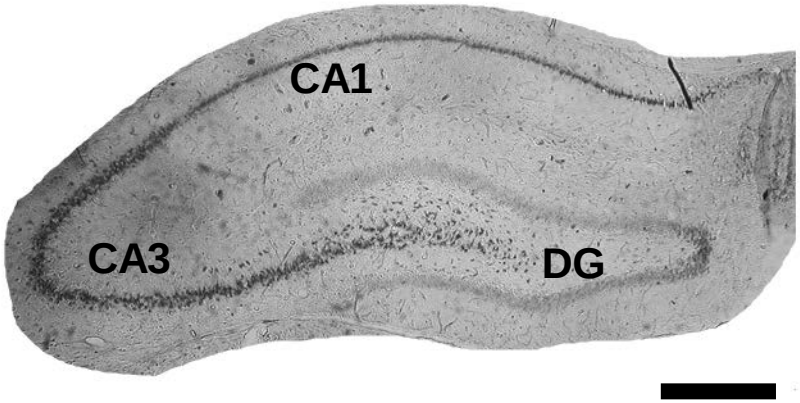

AR

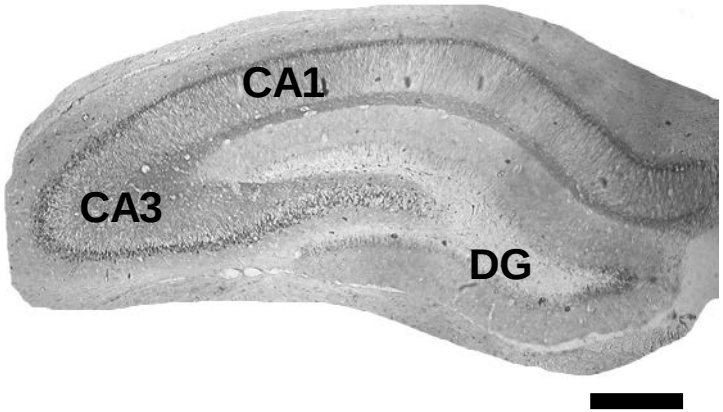

PSD-95

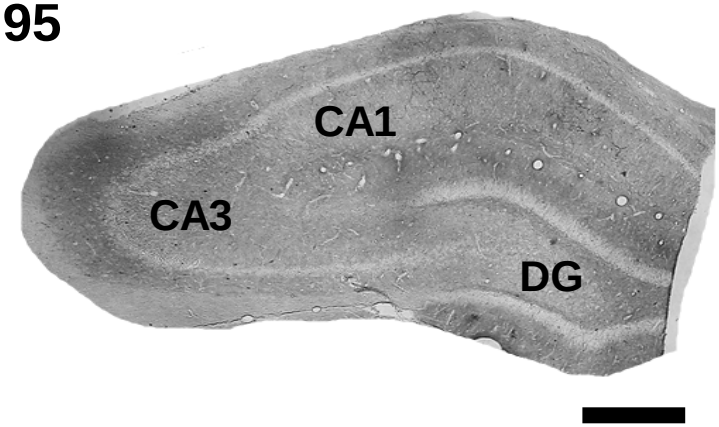

Table. S1 The intra- and inter-assay of accuracy and precision as well as the limit of quantification (LOQ) for each steroid.

	m/z[b] transition	spike [pg]	Intraassay (n[a] = 5) Accuracy (%)	RSD[c] (%)	Interassay (n[a] = 3) Accuracy (%)	RSD (%)	LOQ[d] (pg/0.1g)
T	from 394 to 253	1	111.7	3.0	94.5	2.8	1
		10	102.6	3.3	98.8	3.5	
		100	100.3	1.1	100.4	1.4	
DHT	from 396 to 203	1	108.1	2.6	96.4	5.3	1
		10	98.8	2.3	97.7	3.8	
		100	95.3	3.1	100.7	3.6	
E2	from 558 to 339	0.3	95.3	7.4	93.3	10.0	0.3
		5	97.2	3.6	96.6	5.2	
		20	100.3	3.9	99.9	2.6	

Blank samples, prepared alongside hippocampal samples through the shole extraction and purification procedures, wre spiked with T or other steroids at 0.1, 0.3, 1, 2, 5, 10, 20 and 100 pg, and contents were determined by LC-MS/MS. Accurace was expressed as a percentage of an analytical recovery rate of measured steroid content against spike amount.

[a]For each condition, intra- and interassa were performed five and three items, respectively.

[b]m and z represent the mass and charge of a steroid deriavtive, respectively.

[c]relative standard deviation

[d]LOQ is expressed as pg/0.1 g. Because the average weight of one whole adult hippocampus (0.14 g) was close to 0.1 g, these LOQ values indicate the limit of quantification of steroids from nerly one hippocampus.

Table S2A Primers

Enzyme/Protein name	Gene name	Accession No.	Direction	Primer Sequence (5' to 3')	Primer Length	Product Length [bp*1]	Ta(°C)*2	PCR cycles	Exponetial *3 Amplification
P450scc	*Cyp11a1*	NM_017286	forward	5'-TGACCTATTCCGCTTTGCCTTTGAGT-3'	26-mer	363	62	40	36-42
			reverse	5'-TCTGTGATGTTGGCCTGGATGTTCTT-3'	26-mer				
3β-HSD I	*3β-HSD I*	NM_001007719	forward	5'-AGGGCATCTCTGTTGTCATCCAC-3'	23-mer	275	63	42	40-44
			reverse	5'-TGCCTTCTCGGCCATCCTTT-3'	20-mer				
P450(17α)	*Cyp17a1*	NM_012753	forward	5'-TGGGGCGGGCATAGAGACAACT-3'	22-mer	477	62	33	30-36
			reverse	5'-AGCAAGGCCGTGAAGACAAAGAGC-3'	24-mer				
17β-HSD1	*Hsd17b1*	NM_012851	forward	5'-ACTCCGGGCGTGTGCTGGTGA-3'	21-mer	517	65	30	28-32
			reverse	5'-GGCGTGTCTGGATCCCCTGAAACTT-3'	25-mer				
17β-HSD3	*Hsd17b3*	NM_054007	forward	5'-CTCCCCAACCTGCTCCCAAGTCATTT-3'	26-mer	408	65	31	29-33
			reverse	5'-AGCAAGGCAGCCACAGGTTTCAGC-3'	24-mer				
5α-reductase1	*Srd5a1*	NM_017070	forward	5'-ACCGCGTCCTGCTGGCTATGTTT-3'	23-mer	318	63	25	23-27
			reverse	5'-GGCCTCCCCTGGGTATCTTGTATCC-3'	25-mer				
5α-reductase2	*Srd5a2*	NM_022711	forward	5'-AGGTGGCTTGTTTACGTATGTCTCTG-3'	26-mer	453	57	32	29-35
			reverse	5'-GGCCTCTGTGAAGCTCCAAAAG-3'	22-mer				
P450arom	*Cyp19*	NM_017085	forward	5'-CTGATCATGGGCCTCCTCCTG-3'	21-mer	276	58	32	30-34
			reverse	5'-CCCACGCTTGCTGCCGAATCT-3'	21-mer				
AR	*Ar*	NM_012502	forward	5'-CAACTTTCCGCTCGCTCTGTC-3'	21-mer	536	56	26	24-28
			reverse	5'-TCTGGGGTGGGAAGTAATAGTCG-3'	23-mer				
ERα	*Esr1*	NM_012689	forward	5'-GCCGGCTGCGCAAGTGTTACG-3'	21-mer	467	68	28	26-30
			reverse	5'-GGAGCGCCAGACCAGACCAATCA-3'	23-mer				
ERβ	*Esr2*	NM_012754	forward	5'-GCAAACCAGGAGGCAGAAAGTAGC-3'	24-mer	591	58	28	26-30
			reverse	5'-AAGTGGGCAAGGAGACAGAAAGTAAGTA-3'	28-mer				
PR	*Pgr*	NM_022847	forward	5'-TGAATGAGCAGAGGATGAAGGAGTTG-3'	26-mer	353	60	25	22-26
			reverse	5'-CAGTGCCCGGGATTGGATG-3'	19-mer				
Gapdh	*Gapdh*	NM_017008	forward	5'-TATGACTCTACCCACGGCAAGTTCAA-3'	26-mer	830	60	18	16-24
			reverse	5'-ACCACCCTGTTGCTGTAGCCATATTCAT-3'	28-mer				

*1 bp: base pair

*2 Ta: annealing temperature

*3 PCR cycle numbers for the exponential amplification, estimated from the PCR amplification curves obtained by a number of PCR series using the 3m hippocampal cDNA templates (equivalent to 200 ng (for *Hsd3b1*),).

Table S2B Primers

Enzyme/Protein name	Gene name	Accession No.	Direction	Primer Sequence (5' to 3')	Primer Length	Product Length [bp*1]	Ta(°C)*2	PCR cycles	Exponetial *3 Amplification
StAR	*Star*	NM_031558	forward	5'-CTGGTGGGGCCCCGAGACTT-3'	20-mer	360	60	32	28-34
			reverse	5'-CAATGGCGTGCAGGTAGATGTGGT-3'	24-mer				
TSPO	*Tspo*	NM_012515	forward	5'-GGCTATGGTTCCCTTGGGTCTCTACAC-3'	28-mer	362	63	28	26-30
			reverse	5'-AGGCCCAATGGTCATGAAAGCAGGAT-3'	26-mer				
BDNF	*Bdnf*	NM_001270630	forward	5'-AGGGGCATAGACAAAAGGCACTG-3'	23-mer	403	59	23	21-25
			reverse	5'-AACGGCAACAAACCACAACATTAT-3'	24-mer				
Brain-Insulin1	*Brain-Ins1*	NM_019129	forward	5'-ACCCAAGTCCCGTCGTGAAGT-'3	21-mer	164	57	36	34-38
			reverse	5'-CCAGTTGGTAGAGGGAGCAGATG-3'	23-mer				
SIRT1	*Sirt1*	NM_001107627	forward	5'-GACTGGAGCTGGGGTTTCTGTTT-3'	23-mer	231	60	33	30-34
			reverse	5'-ATGCTGAGTTGCTGGATTTTGTGT-3'	24-mer				
p53	*Tp53*	NM_030989	forward	5'-GGCCCGCACCCTACTTCCC-3'	19-mer	149	62	30	26-32
			reverse	5'-TATCATCTGGAGGAAGAAGTTTC-3'	23-mer				

*1 bp: base pair

*2 Ta: annealing temperature

*3 PCR cycle numbers for the exponential amplification, estimated from the PCR amplification curves obtained by a number of PCR series using the 3m hippocampal cDNA templates (equivalent to 200 ng (for *Hsd3b1*),).